ORNL-3555
UC-80 – Reactor Technology
TID-4500 (26th ed.)

AN EXPERIMENTAL INVESTIGATION OF INSTANTANEOUS-COLLAPSE AND CREEP-BUCKLING CHARACTERISTICS OF CYLINDRICAL SHELLS

B. L. Greenstreet
J. M. Corum

OAK RIDGE NATIONAL LABORATORY
operated by
UNION CARBIDE CORPORATION
for the
U.S. ATOMIC ENERGY COMMISSION

Printed in USA. Price: $1.00 Available from the
Office of Technical Services
U. S. Department of Commerce
Washington 25, D. C.

ORNL-3555

Contract No. W-7405-eng-26

Reactor Division

AN EXPERIMENTAL INVESTIGATION OF INSTANTANEOUS-COLLAPSE AND CREEP-BUCKLING CHARACTERISTICS OF CYLINDRICAL SHELLS

B. L. Greenstreet
J. M. Corum

MARCH 1964

OAK RIDGE NATIONAL LABORATORY
Oak Ridge, Tennessee
operated by
UNION CARBIDE CORPORATION
for the
U. S. ATOMIC ENERGY COMMISSION

THIS PAGE

WAS INTENTIONALLY

LEFT BLANK

CONTENTS

AN EXPERIMENTAL INVESTIGATION OF INSTANTANEOUS-COLLAPSE AND CREEP-BUCKLING CHARACTERISTICS OF CYLINDRICAL SHELLS

B. L. Greenstreet
J. M. Corum

Abstract

Instantaneous-collapse and creep, or time-dependent, buckling tests were conducted on nominally 8.0-in.-OD by 0.25-in.-wall and 4.0-in.-OD by 0.12-in.-wall specimens made from commercial pipe and tubing. The material for the larger specimens was type 304 stainless steel, while the smaller ones were made of both type 304 and type 347 stainless steel. The length chosen in each case was infinite from the buckling standpoint. The instantaneous-collapse test temperatures ranged from room temperature to 1200°F, and all the time-dependent collapse tests were made at 1200°F.

The results show that tube out-of-roundness is a major factor in determining the collapse pressure. They also show that, under creep-collapse conditions, the critical pressure decreases rapidly with time, initially. This decrease is then followed by a leveling off, with very little change after the first few hundred hours. Although the load-carrying abilities of the 8.0-in.-OD specimens exceeded those for 4.0-in.-OD specimens of the same material for instantaneous and short-time collapse conditions, the critical pressures were about the same in the two cases for collapse after several hundred hours. The ratio of experimental values to the allowable working pressure given by the ASME Boiler and Pressure Vessel Code, Section VIII, Rules for Construction of Unfired Pressure Vessels, ranges from about 6.0 for instantaneous buckling to about 3.4 at 3400 hr in the case of the 8.0-in.-OD tubes. For the 4.0-in.-OD type 304 stainless steel tubes, the ratio is about 4.5 for instantaneous buckling and about 3.4 for buckling after a few thousand hours.

Introduction

In cases in which shell structures are subjected to sustained external loads at temperatures where creep of the material is important, creep buckling may occur. Theoretically, a thin shell held under creep conditions and subjected to an external pressure loading will collapse after a finite interval of time, even when the pressure is much below the instantaneous buckling pressure. Thus the creep-buckling characteristics of a vessel subjected to external pressure loadings are important in assessing its structural adequacy for a given application.

Section VIII of the ASME Boiler and Pressure Vessel Code gives rules for the design of vessels subjected to external pressure at temperatures in the creep ranges for the materials. However, the rules are based on instantaneous-collapse predictions, and, although factors of safety of 4 for cylindrical shells and about 5.8 for hemispherical shells are included, the magnitudes of these factors for creep buckling, or time-dependent collapse, are unknown. It is known that the values decrease with time under load.

Experiments on the creep buckling of shell structures have been conducted, but many of the tests were for specialized cases or were made using machined specimens where the dimensions were carefully controlled. Basic information regarding the buckling phenomena were derived from these tests, and theories for predicting the load-carrying abilities of shells have been advanced. Despite these facts, the designer cannot make accurate predictions, on the basis of the information now available regarding the creep, or time-dependent, buckling behavior of a particular shell structure. Neither can he infer the amount of conservatism associated with Code-allowable pressures in the presence of creep-buckling conditions.

In view of these facts, a study was made to determine the collapse characteristics of specimens made from commercial, seamless tubing. Instantaneous and time-dependent collapse tests on nominally 8.0-in.-OD by 0.25-in.-wall and 4.0-in.-OD by 0.12-in.-wall specimens were conducted. The material for the larger specimens was type 304 stainless steel. The smaller ones were made using both type 304 and type 347 stainless steel so that the behavior of the two materials could be compared. The specimen lengths were approximately 9 ft for the 8.0-in.-OD specimens and 5 ft for the 4.0-in.-OD ones; these lengths are infinite from the buckling standpoint. Although this study was not comprehensive because of the limited number of specimens and ranges of variables, much information regarding the buckling phenomenon was gained.

The test procedures and results are described in the following sections. A method for making theoretical analyses was also derived, and test results were compared with calculated values. Both the theoretical model and additional comparisons of the predicted values with experimental results are given in a separate report.[1] Application of the results to the design of the through-tubes for the experimental loops in the Experimental Gas-Cooled Reactor being constructed at Oak Ridge, Tennessee, is given in the Appendix.

Experimental Procedures

The 8.0-in.-OD tubes were tested in an electrically heated autoclave that has a maximum rating of 600 psi at 1400°F. Heaters were initially installed inside the cylindrical pressure vessel. This vessel has an inside diameter of 12 in., an outside diameter of 16 1/4 in., and is made of type 316 stainless steel. The test chamber is 124 in. long, and, with the heaters mounted inside the vessel, the diameter is 10 in. Following the first test, the heaters mounted inside the vessel were replaced by Calrod heaters attached on the outside.

A 6 1/2-in.-OD insert was used inside the test specimens to prevent jamming inside the autoclave as a result of excessive deformation. Two separate alarm systems were used to indicate collapse. The first utilized an electrical circuit that rang an alarm bell when the specimens made contact with the steel insert. The second was activated by the pressure increase resulting from a volume change in the annulus between the specimens and the insert. Helium was used to apply the external pressure. By carefully insulating the autoclave and regulating the heat input in various regions, the temperature spread along each specimen was held to within a 50°F range, except in the first case, as described later. The temperature fluctuations at any point with time were also held within a 50°F range.

All the seamless tubing for the 8.0-in.-OD, 0.25-in.-wall specimens was from the same heat of type 304 stainless steel. This tubing was manufactured in accordance with ASTM-A213-58T specifications. Five specimens

[1] J. M. Corum, "An Investigation of the Instantaneous and Creep Buckling of Initially Out-of-Round Tubes Subjected to External Pressure," USAEC Report ORNL-3299, Oak Ridge National Laboratory, Jan. 16, 1963.

were tested. Four were tested at a temperature of 1200°F. Two of these were collapsed instantaneously, while two underwent time-dependent, or creep, collapse.

In conducting the 1200°F tests, the system was initially pressurized to about 50 psi with helium; the autoclave was then brought up to temperature. After the temperature was stabilized, the pressure was gradually increased until either the specimen collapsed or the desired test pressure was reached.

To obtain more insight regarding the collapse mechanism, the fifth 8.0-in.-OD tube was instrumented with strain gages and collapsed at room temperature. Circumferential gages were located at two axial locations and at 22.5-deg increments around the tube circumference at each axial location. The outside gages, which were exposed to external pressure, were 1/4-in. gage-length Tatnall Metalfilm, temperature-compensated, C9-141 epoxy-back gages. Baldwin SR-4, type A-7, paper-backed wire gages with a 1/4-in. gage length were used on the inside of the tube. Hydraulic oil was used to apply the external pressure, and the strains were recorded at selected pressure increments.

The tests on the 4.0-in.-OD specimens were conducted by the University of Tennessee. Again, an electrically heated autoclave was used. This autoclave was a cold-wall type of furnace made from 10-in. extra-strong carbon-steel pipe with clam-shell heaters mounted inside. Silicell C-3 insulation was used in the annulus between the heaters and the furnace wall. The inside diameter of the heaters was 5.0 in., and the length of heated chamber was 12 ft.

The pressurizing gas for these tests was also helium. A 3 1/2-in.-OD insert was used inside the specimens, and the two alarm systems described above for the 8.0-in.-OD tube tests were used to signal collapse. During each test, the temperature spread was held to within ±50°F of the specified value, except for three of the specimens. The temperature variations on these latter specimens are discussed in the next section. The temperature fluctuations at any point with time were limited to ±20°F.

The 4.0-in.-OD, 0.12-in.-wall specimens were made from two different materials, as mentioned earlier. Four were made from type 304 stainless steel, while two were made from type 347. The stock material for all the specimens was manufactured in accordance with ASTM-A312-58T specifications for pipe. In this case, seamless pipe was used. The nominal specimen temperature at the time of collapse was 1200°F in all cases, except for the type 347 stainless steel specimens.

In the first test, two specimens, one of each type of material, were mounted in the furnace and collapsed instantaneously. Only one tube was mounted in the furnace for each of the subsequent tests, which included creep-buckling tests on two type 304 stainless steel units and instantaneous-collapse tests on the remainder. At the beginning of a test, the inside of the specimen (or specimens) was evacuated and filled with helium to a pressure of approximately 15 psi. The furnace was then evacuated and filled with helium to a pressure of about 100 psi. Following this, the furnace was heated slowly to the desired temperature while simultaneously bleeding the tube pressure to 10 psi. The pressure in the furnace was then gradually increased by small additions of helium so that the associated temperature fluctuations were small.

Dimensional data were obtained on all the 8.0-in.-OD and 4.0-in.-OD specimens prior to testing them. The outside diameters and wall thicknesses of each tube were measured at 1-ft intervals along the tube axis and at angular intervals around the circumference at each axial location. The diameters were measured at 30-deg intervals on all the 8.0-in.-OD specimens and on the last 4.0-in.-OD, type 304 stainless steel specimen. The interval was 60 deg on the remaining 4.0-in.-OD tubes. Specimens subjected to creep buckling were also measured at different time intervals during each test.

In every specimen the initial cross section at each axial location was found to be quasi-elliptical in shape, and an out-of-roundness factor was calculated for each location. The percentage wall thickness variation at each location was also calculated.

Experimental Results

Tests of 8.0-in.-OD, 0.25-in.-Wall Specimens

The 8.0-in.-OD specimens were designated RD-1 through -5. In collapsing the first specimen, limitations on heater control imposed by the furnace design precluded elimination of temperature gradients along the length of the specimen. The average temperatures along the unit immediately prior to collapse are shown in Fig. 1; the positions at which the diameter and wall thickness were measured before collapse are also shown.

The collapsed specimen is shown in Fig. 2. The thermocouples used to record the specimen temperatures may be seen on the tube. It collapsed into an elliptical shape with two bulges extending outward beyond the original circular form and two extending inward to form two lobes. The most pronounced change in shape occurred in the region that was at a temperature of 1200°F. This portion of the collapsed tube is shown in Fig. 3.

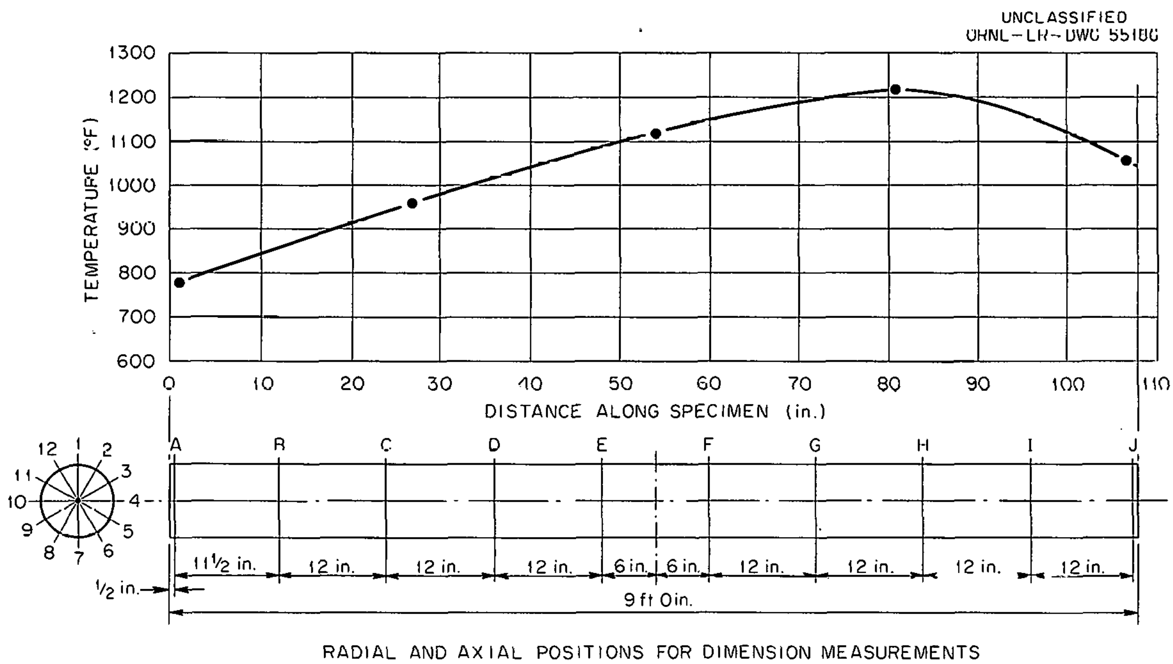

Fig. 1. Axial Temperature Distribution Along Specimen RD-1 at Time of Collapse and Diagram of Positions at Which Diameter and Wall Thickness Were Measured Before Collapse.

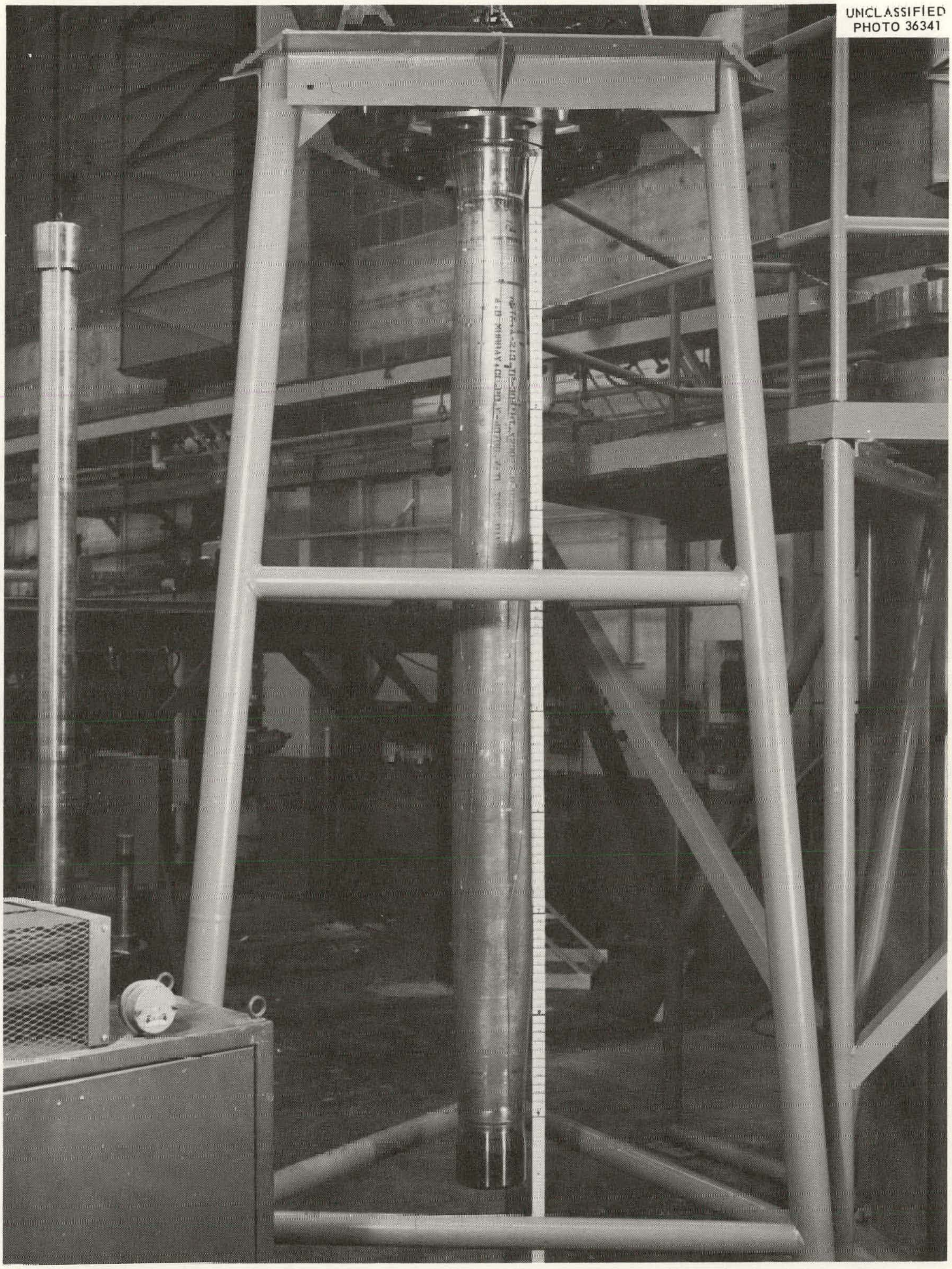

Fig. 2. Collapsed 8.0-in.-OD, 0.25-in.-Wall Type 304 Stainless Steel Specimen RD-1.

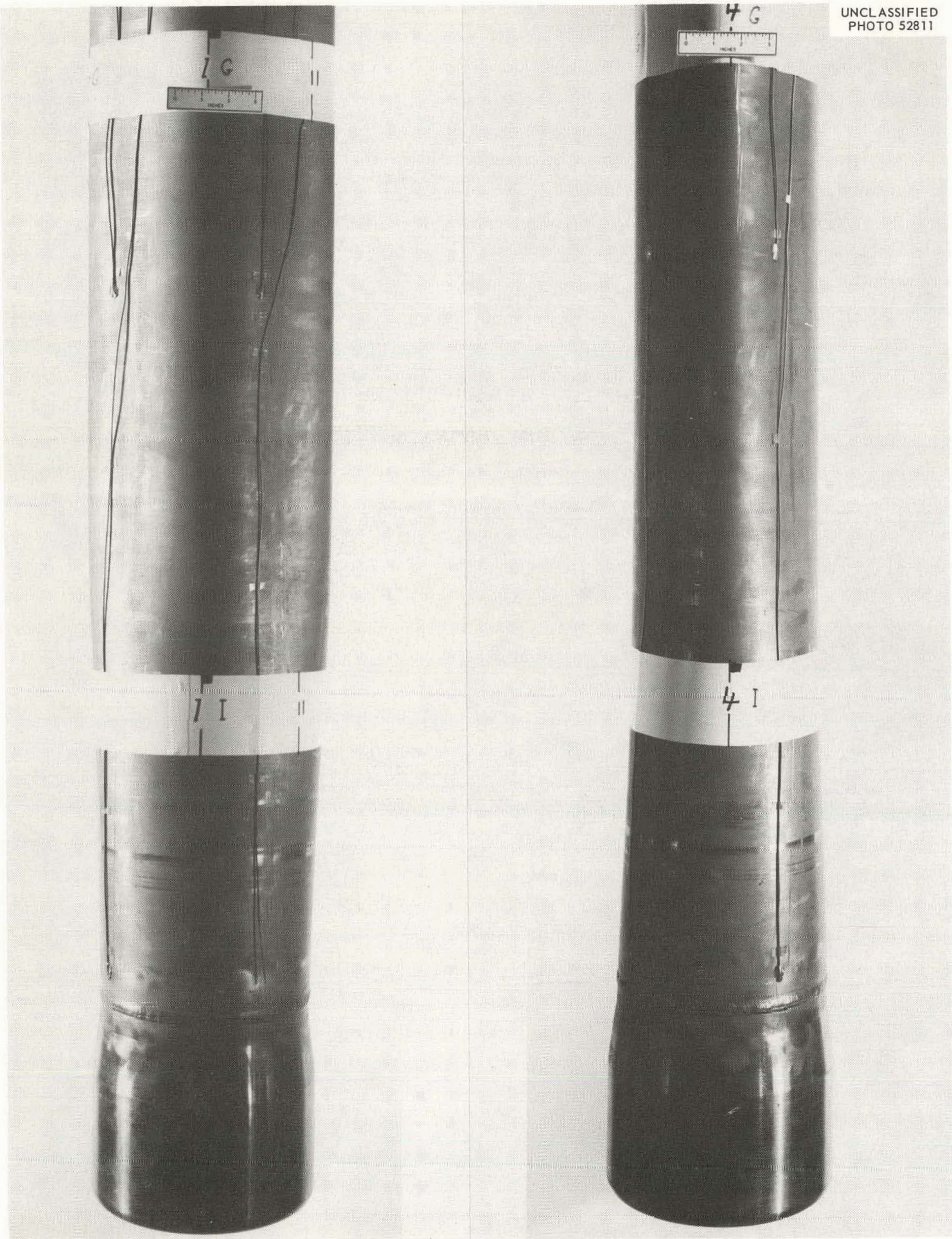

Fig. 3. Portion of Collapsed Specimen RD-1 that Was Subjected to the Highest Temperature.

The critical pressure was 805 psi, and the location of the maximum deformation indicated that the pressure was close to the value to be expected for a tube held uniformly at 1200°F. Because of variations in materials properties with temperature, the axial temperature gradient probably had an effect similar to the end effects for a short tube.

The heaters inside the furnace were subsequently replaced with zone-controlled Calrod heaters mounted on the outside of the furnace. With these heaters and additional insulation around the top head of the autoclave, much more uniform temperatures were obtained during the remaining tests.

Each of the remaining tubes that were tested at 1200°F (RD-2, -3, and -4) collapsed into the characteristic two-lobe mode described above. As an additional example of the appearance after failure, a postcollapse photo of RD-2 is shown in Fig. 4. The autoclave used in testing the 8.0-in.-OD tubes may be seen in the background of this picture with insulation on the outer surface. The dimensional data and collapse conditions for the four tubes are given in Table 1, where it may be seen that the critical pressures for the two specimens collapsed under the same conditions compare favorably.

The out-of-roundness factor, η, is given by

$$\eta = \frac{OD_{max} - OD_{min}}{4h} ,$$

where h is the average wall thickness. The average out-of-roundness factor for each tube is obtained by averaging the values for the axial locations, while the maximum out-of-roundness factor is the maximum of several values for the tube.

The positive wall thickness variation at each axial location is given by

$$\% \text{ positive variation} = \left(\frac{\text{max wall thickness} - \text{avg wall thickness}}{\text{avg wall thickness}}\right) \times 100 .$$

For a negative variation, the minimum wall thickness is used. The average wall thickness variations given in the table are the averages of all values for a tube.

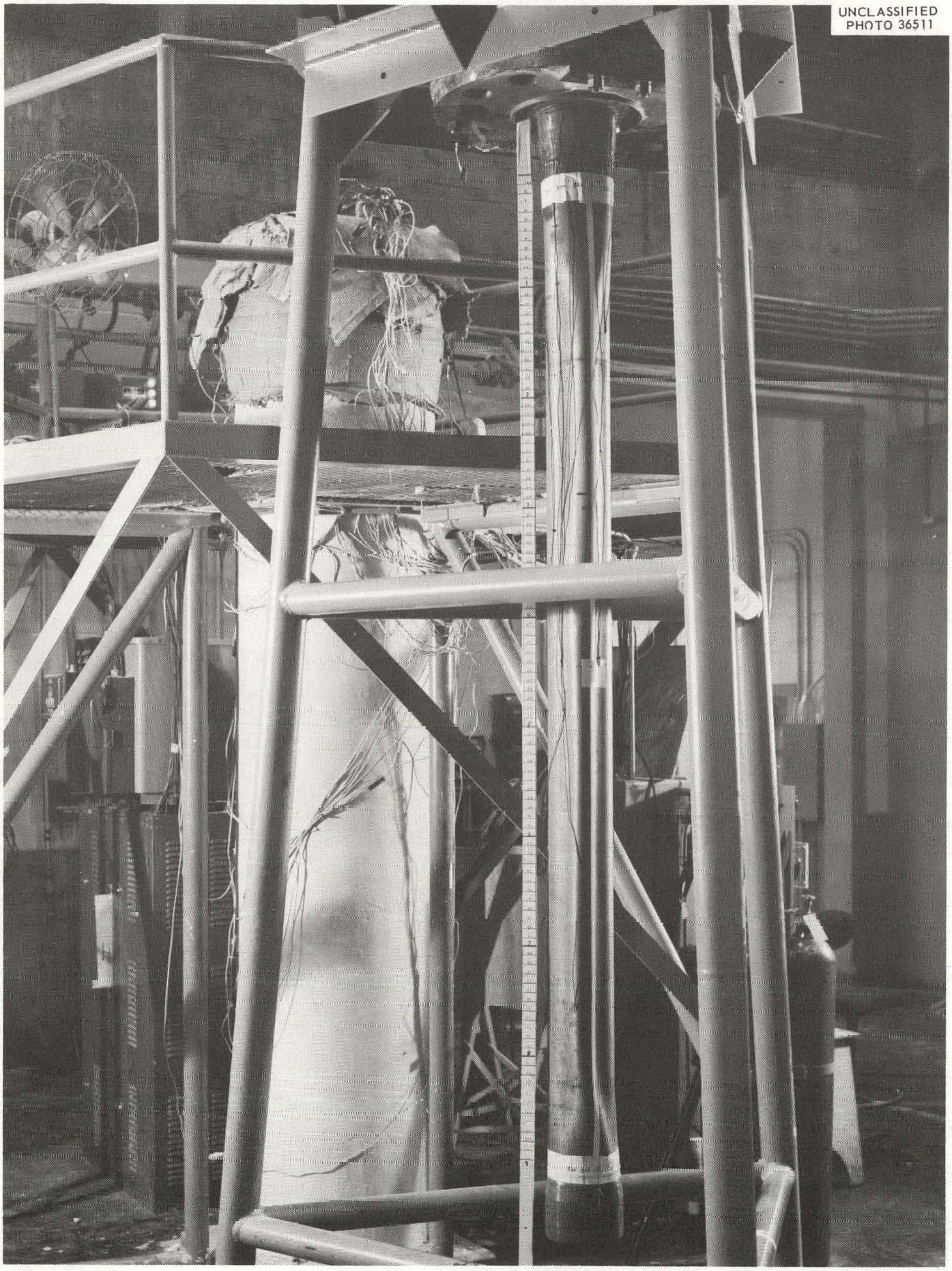

Fig. 4. Collapsed 8.0-in.-OD, 0.25-in.-Wall Type 304 Stainless Steel Specimen RD-2.

Table 1. Dimensional Data and Collapse Conditions for 8.0-in.-OD, 0.250-in.-Wall, Type 304 Stainless Steel Tubes Collapsed at a Temperature of 1200°F

	Specimen RD-1	Specimen RD-2	Specimen RD-3	Specimen RD-4
Average measured mean radius-to-thickness ratio, a/h	15.02	15.83	15.71	15.40
Average measured wall thickness, in.	0.258	0.245	0.247	0.252
Average out-of-roundness factor	0.025	0.036	0.032	0.023
Maximum out-of-roundness factor	0.041	0.184	0.182	0.035
Average positive wall-thickness variation, %	4.72	5.36	5.57	5.95
Average negative wall-thickness variation, %	−4.56	−5.51	−5.63	−5.86
External collapse pressure, psi	805	780	595	460
Time to collapse, hr	~0	~0	60	3410

The initial variations in outside diameter and wall thickness at each axial location are depicted in Figs. 5, 6, and 7 for specimens RD-1, RD-2, and RD-3, respectively. A circle was chosen to represent the nominal 8.0-in. outside diameter, and the actual diameter, in each case, was drawn by greatly magnifying the deviations from the nominal diameter. A second circle was chosen to represent the nominal inside diameter, and the wall-thickness variations from the nominal 0.250 in. were plotted from this circle. The approximate orientation of the cross section of the collapsed tube at each axial position is sketched in the center of each of the plots in Figs. 5, 6, and 7. A comparison of the out-of-roundness, the wall-thickness variation, and the orientation of the collapse pattern may be made by examining these figures. For each of the 8.0-in.-OD specimens tested, the cross-sectional configuration after collapse can be correlated directly with the initial out-of-roundness.

The cross-sectional configurations for the time-dependent collapse specimens were not as distorted after collapse as were those of the instantaneously collapsed tubes. The differences in distortion occurred

UNCLASSIFIED
ORNL-LR-DWG 66533

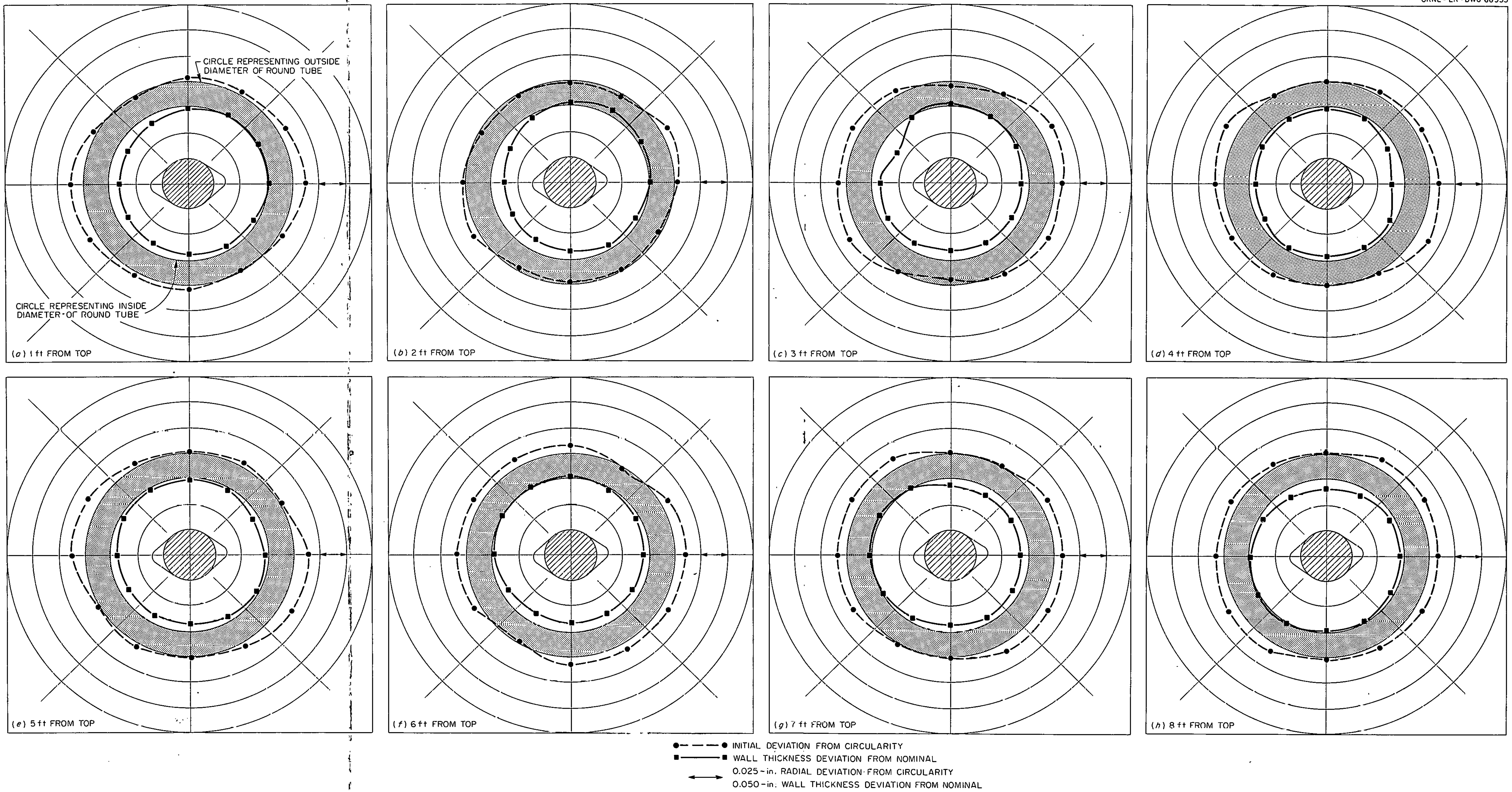

Fig. 5. Exaggerated Initial Dimensional Variations of Tube-Collapse Specimen RD-1.

UNCLASSIFIED
ORNL-LR-DWG 66534

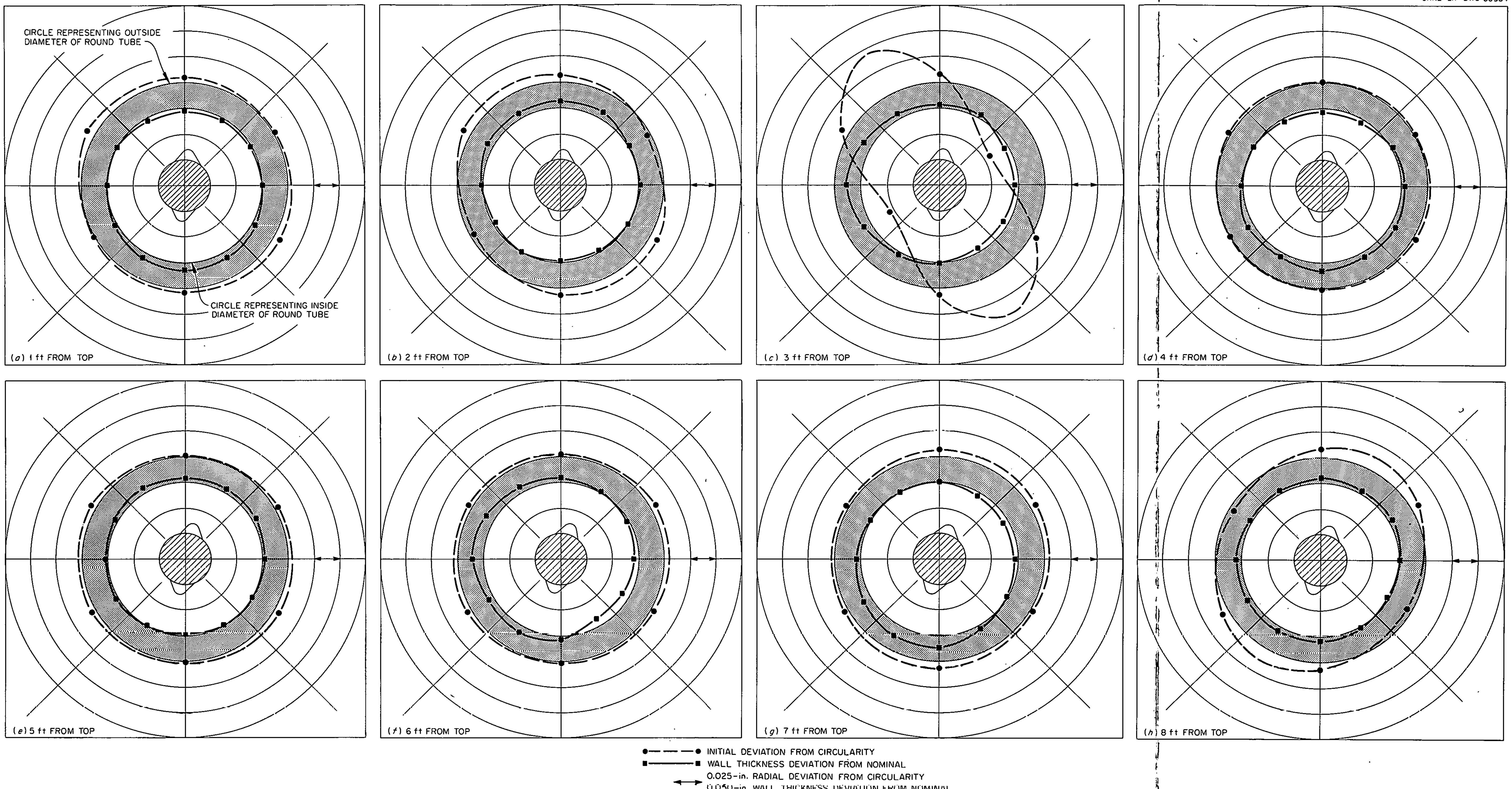

Fig. 6. Exaggerated Initial Dimensional Variations of Tube-Collapse Specimen RD-2.

UNCLASSIFIED
ORNL-LR-DWG 66535

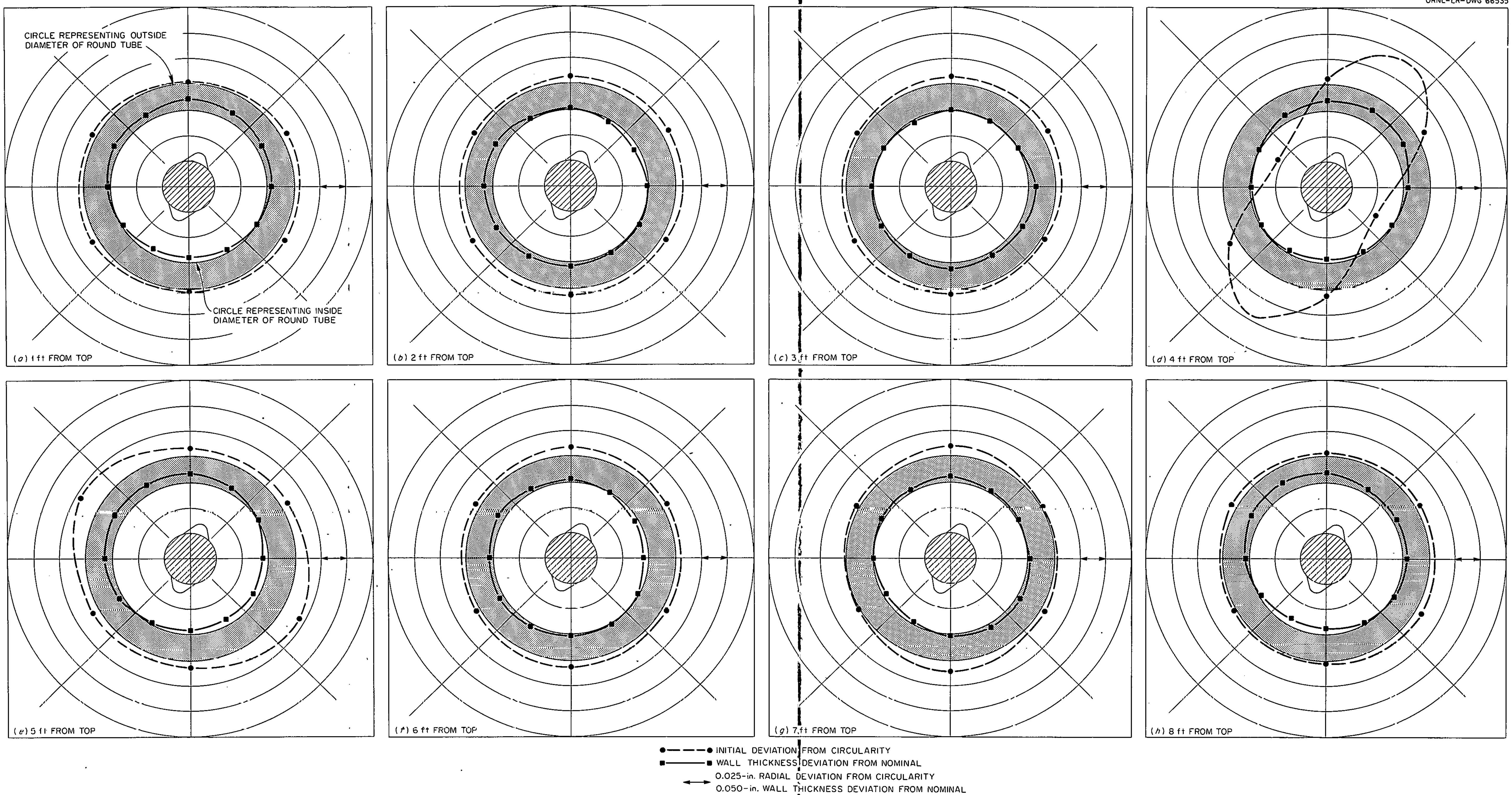

Fig. 7. Exaggerated Initial Dimensional Variations of Tube-Collapse Specimen RD-3.

because of differences in the compressive stresses. The mean compressive stresses in the walls of the tubes that buckled instantaneously exceeded the proportional limit of the material. Thus collapse of the specimens was initiated through inelastic action, and the initial resistance to bending deformation was smaller than it would have been if the mean stress had been below the proportional limit. For the creep-collapse specimen, the mean stress was below the proportional limit, and collapse was initiated through elastic action with subsequent higher initial resistance to deformation.

Specimen RD-4, which was subjected to an external pressure of 460 psi and collapsed after 3410 hr, was removed from the test facility after 1056 and 2168 hr of total test time, and outside-diameter measurements were made at each of the locations where initial measurements were made. By comparing these measurements with the initial measurements, the creep behavior of the tube during the first 2168 hr of the test was examined. This comparison is shown in Fig. 8, together with the initial wall-thickness variations. The orientation of the collapse pattern at each axial location is sketched at the center of each plot. Figure 8 shows the initial quasi-elliptical shape at each cross section, and an examination, in consecutive order, of the plots in the figure shows that the major axis spirals counterclockwise around the tube from top to bottom. Furthermore, this initial ellipticity was simply magnified by creep of the material under the external pressure. The deformation that occurred during the 1112 hr after the 1056-hr measurements were made was considerably less, however, than that which occurred during the first 1056 hr. Although the differences in dimensions for the 1056-hr and the 2158-hr measurements are small, they are greater than or equal to the precision associated with the measurements, and the trend toward greater ellipticity is real. The correspondence between orientation of the final collapse pattern of the tube and the quasi-elliptical deformation may be seen in the figure.

The fifth 8.0-in.-OD, 0.25-in.-wall, type 304 stainless steel tube, RD-5, which was instrumented with electrical resistance strain gages and collapsed at room temperature, was tested in the facility used for the high-temperature tests. No insert was used inside the specimen in this

UNCLASSIFIED
ORNL-LR-DWG 66536

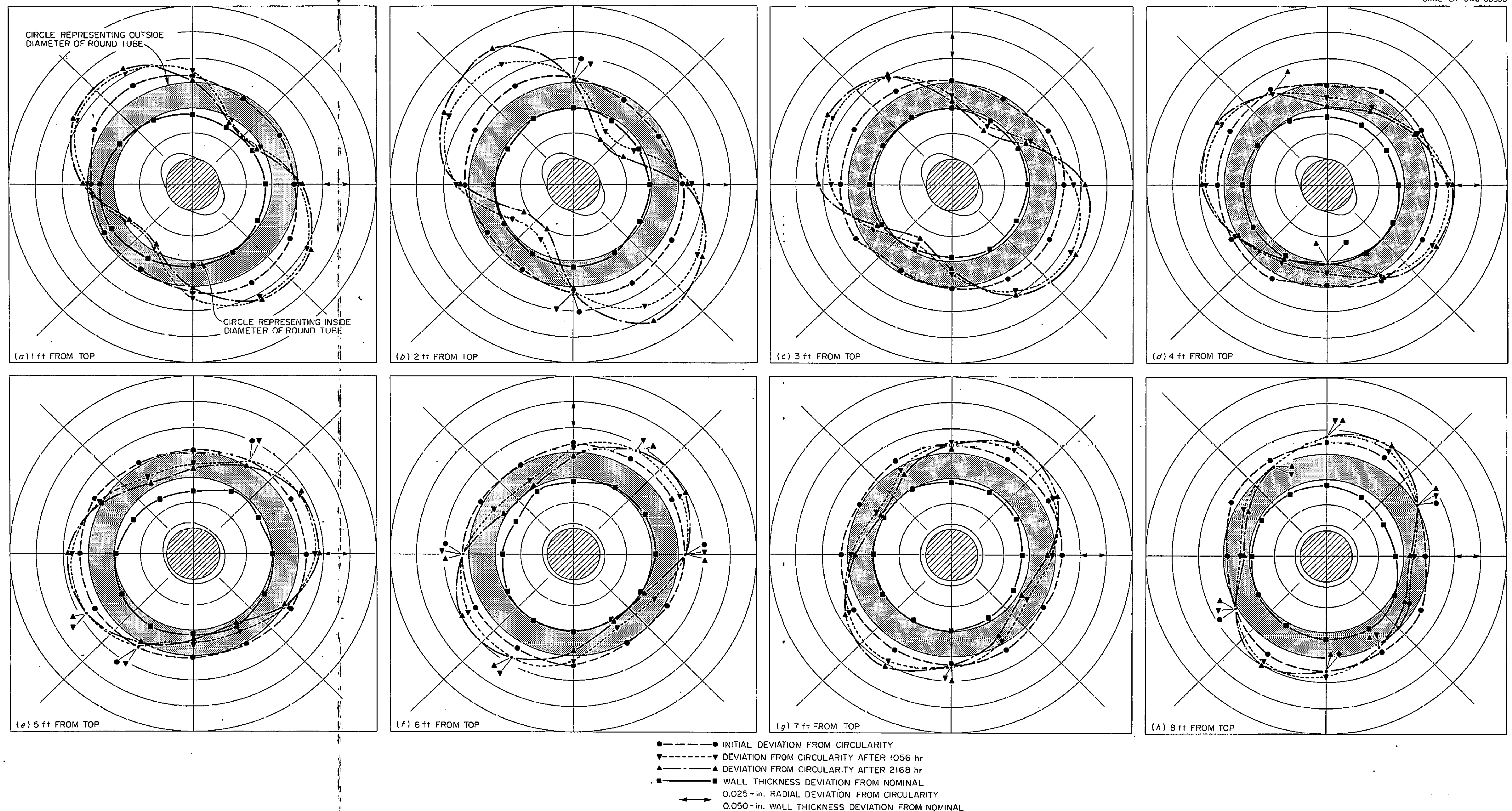

Fig. 8. Exaggerated Initial Dimensional Variations and Creep Deformation of Tube-Collapse Specimen RD-4 Subjected to an External Pressure of 460 psi at 1200°F.

case. The collapse pressure of 1185 psi was lower than expected, possibly because the tube was flattened slightly by the brackets that were clamped to the tube for handling purposes.

The initial dimensional data for the tube are given in Table 2. The initial measured variations in outside diameter and wall thickness are depicted in Fig. 9. Sketches in the center of each plot again depict the orientation of the collapsed cross sections at each axial position. The collapsed tube is shown in Fig. 10. Additional oil was pumped into the test chamber after instability occurred. This accounts for the tube being highly deformed. Figure 10 shows that buckling occurred in a localized region, indicating that some weakening factor was present in that region. No such weakening effect was indicated by the initial dimensional measurements, although the tube did collapse into a two-lobe mode with the same orientation as the initial quasi-elliptical out-of-roundness. A complete description of the test and the strain-gage results are given in ref. 1, pages 53 through 66.

Table 2. Dimensional Data for Room-Temperature Strain-Gaged Collapse Specimen

Average measured mean radius-to-thickness ratio, a/h	15.09
Average measured wall thickness, in.	0.257
Average out-of-roundness factor	0.022
Maximum out-of-roundness factor	0.035
Average positive wall-thickness variation, %	7.93
Average negative wall-thickness variation, %	−6.86

Tests of 4.0-in.-OD, 0.12-in.-Wall Specimens

The dimensional data and collapse conditions for the four 4.0-in.-OD type 304 stainless steel specimens are given in Table 3, and the data for the 4-in.-OD type 347 stainless steel specimens are given in Table 4. A

UNCLASSIFIED
ORNL-LR-DWG 66537

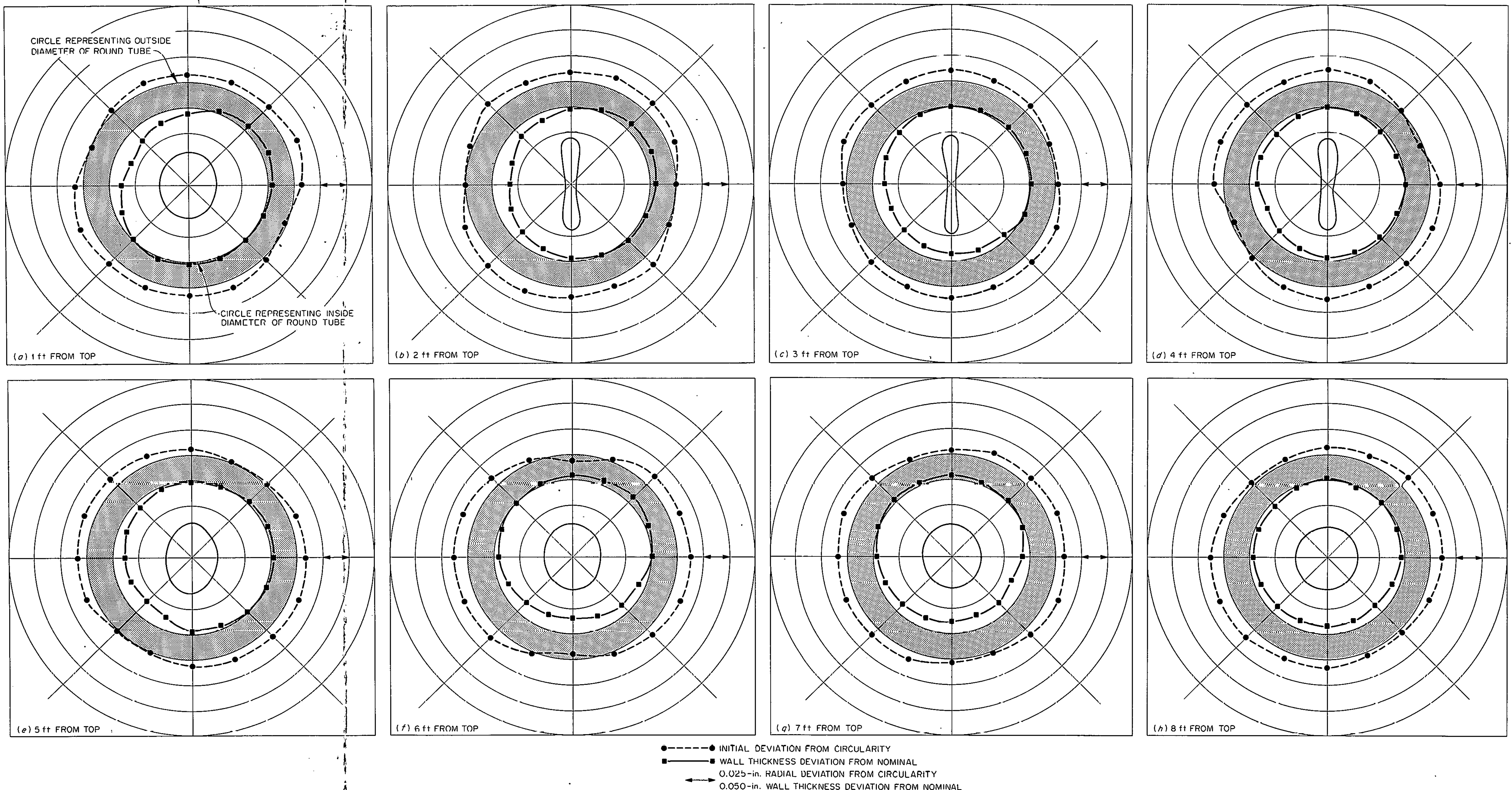

Fig. 9. Exaggerated Initial Dimensional Variations of Room-Temperature Strain-Gaged Collapse Specimen RD-5.

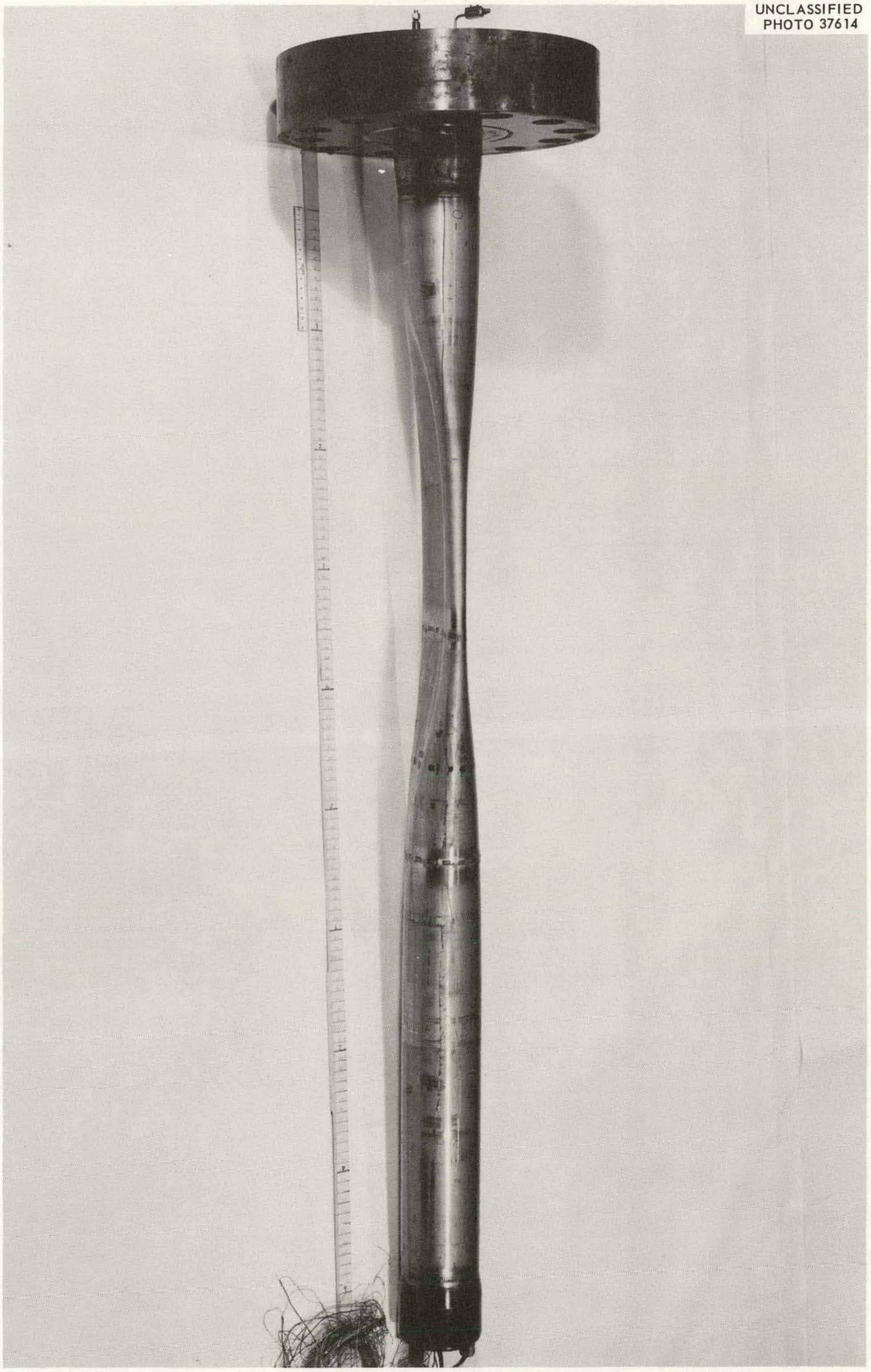

Fig. 10. Collapsed Room-Temperature Strain-Gaged Specimen RD-5.

Table 3. Dimensional Data and Collapse Conditions for 4.0-in.-OD, 0.120-in.-Wall, Type 304 Stainless Steel Tubes Collapsed at a Temperature of 1200°F

	UT-1	UT-3	UT-5	UT-6
Average measured mean radius-to-thickness ratio, a/h	16.30	16.33	15.30	15.48
Average measured wall thickness, in.	0.120	0.119	0.127	0.126
Average out-of-roundness factor	0.007	0.012	0.005	0.009
Maximum out-of-roundness factor	0.009	0.028	0.009	0.013
Average positive wall-thickness variation, %	0.48	5.23	6.21	4.06
Average negative wall-thickness variation, %	−0.48	−5.31	−4.49	−6.23
External collapse pressure, psi	588	542	425	425
Time to collapse, hr	~0	~0	260	>14.160

Table 4. Dimensional Data and Collapse Conditions for 4.0-in.-OD, 0.120-in.-Wall, Type 347 Stainless Steel Tubes

	UT-2	UT-4
Average measured mean radius-to-thickness ratio, a/h	16.24	15.41
Average measured wall thickness, in.	0.120	0.126
Average out-of-roundness factor	0.014	0.005
Maximum out-of-roundness factor	0.022	0.006
Average positive wall-thickness variation, %	0.67	8.84
Average negative wall-thickness variation, %	−0.75	−7.69
External collapse pressure, psi	991	900
Time to collapse, hr	~0	~0

comparison of the out-of-roundness factors listed in Tables 3 and 4 with those in Table 1 shows that these factors were much larger for the 8.0-in.-OD specimens than for the 4.0-in.-OD ones.

The initial variations in outside diameter and wall thickness at each axial location for all specimens, except UT-6, are given in Figs. 11 through 15. The approximate orientation of the cross section of the collapsed tube at each axial location is sketched in the center of each of the plots in Figs. 11 through 15.

The first two test specimens were mounted in the furnace at the same time and collapsed instantaneously. One was made from type 304 stainless steel and designated UT-1, while the other, UT-2, was made from type 347 stainless steel. The type 304 stainless steel tube, which was positioned above the other tube, collapsed under an external pressure of 590 psi while at a uniform temperature of 1200°F. Following the collapse of this tube, the pressure was increased, and the type 347 stainless steel tube failed at a pressure of 990 psi. However, the addition of cold helium during the pressurizing process caused a reduction in temperature in the lower portion of the furnace, with the result that the upper end of the tube was at 1200°F while the temperature at the lower end was 920°F.

The collapsed tubes are shown in Fig. 16, where UT-2 is labeled A and UT-1 is labeled B. These tubes bulged on only one side, and it may be seen from the figure that the angular location of the bulge was different for the upper and lower portions of UT-1. An examination of the plots giving the initial variations in outside diameter and wall thickness (Figs. 11 and 12) reveals some correlation between collapsed geometry and original variations.

The next three tubes in this test series (UT-3, -4, and -5) also collapsed with a single bulge. The thinner regions of the tube walls moved outward to form the bulge. The second type 347 stainless steel tube (UT-4) was collapsed while the temperature was 1200°F at one end, 1170°F at the center, and 1130°F at the other end. Specimen UT-5, which was subjected to a pressure of 425 psi, collapsed in the region of minimum wall thickness, which was near one end. This occurred at the end of 260 hr. The test was

UNCLASSIFIED
ORNL-LR-DWG 70525

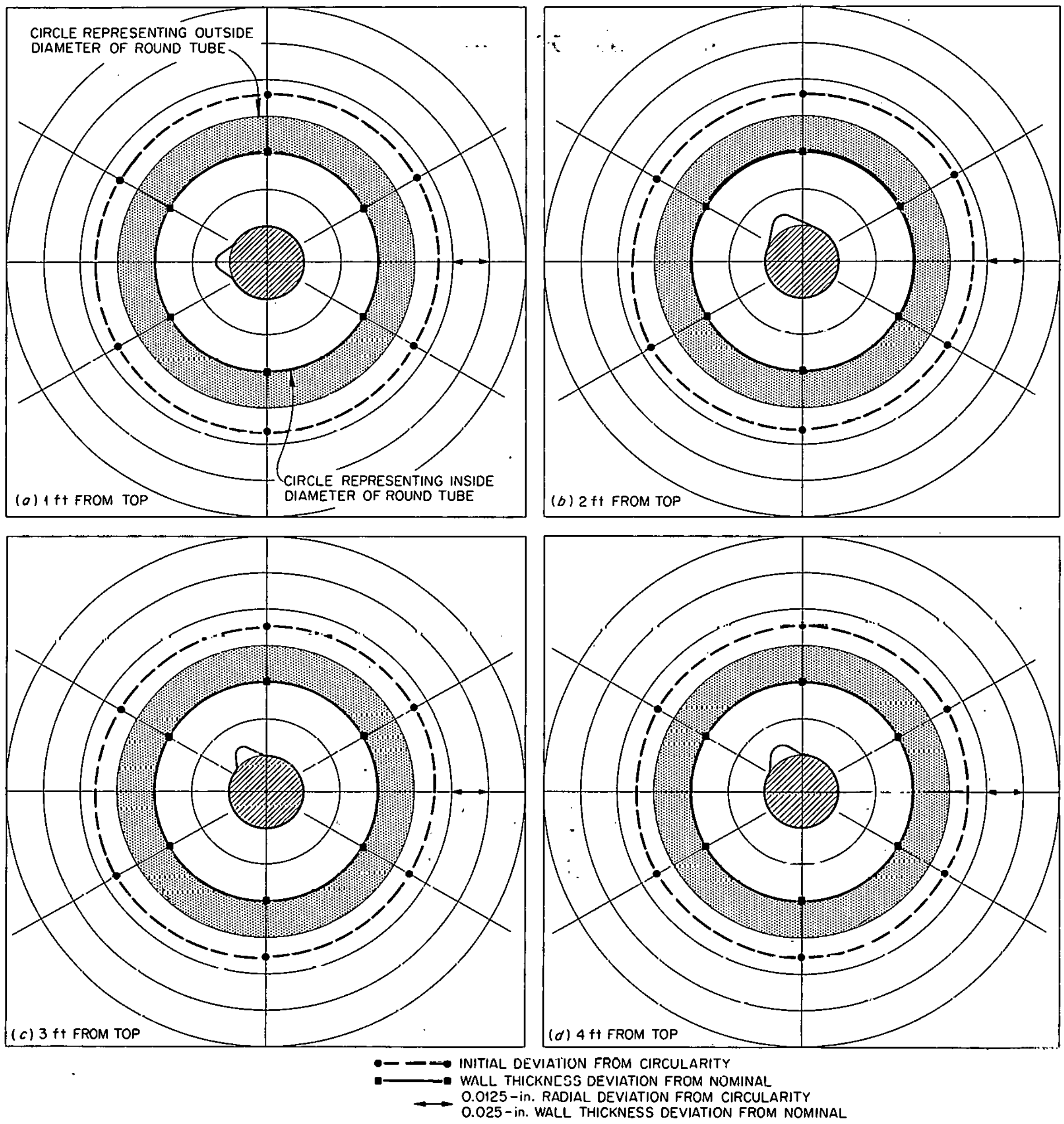

Fig. 11. Exaggerated Initial Dimensional Variations of Tube-Collapse Specimen UT-1.

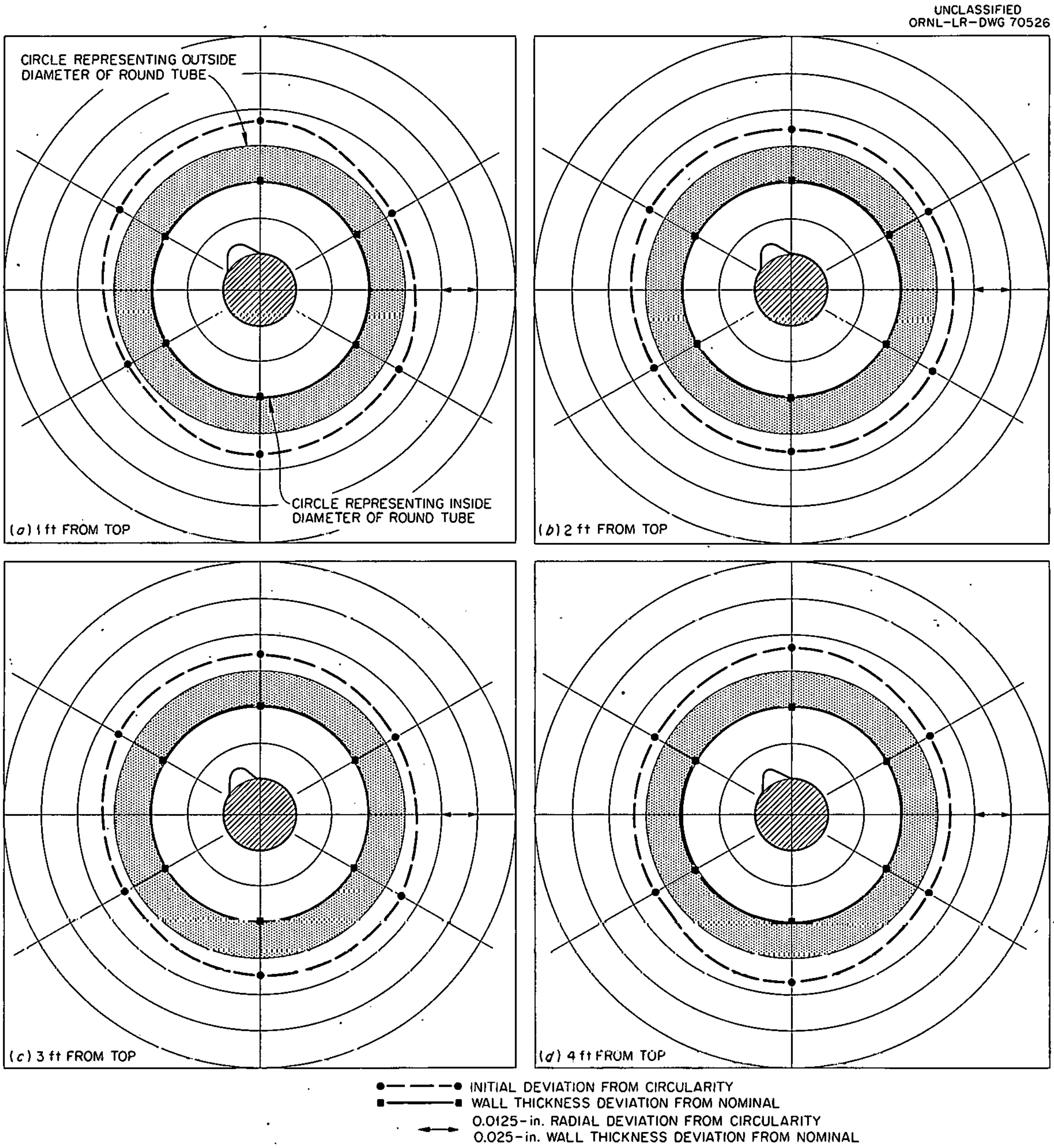

Fig. 12. Exaggerated Initial Dimensional Variations of Tube-Collapse Specimen UT-2.

UNCLASSIFIED
ORNL-LR-DWG 70527

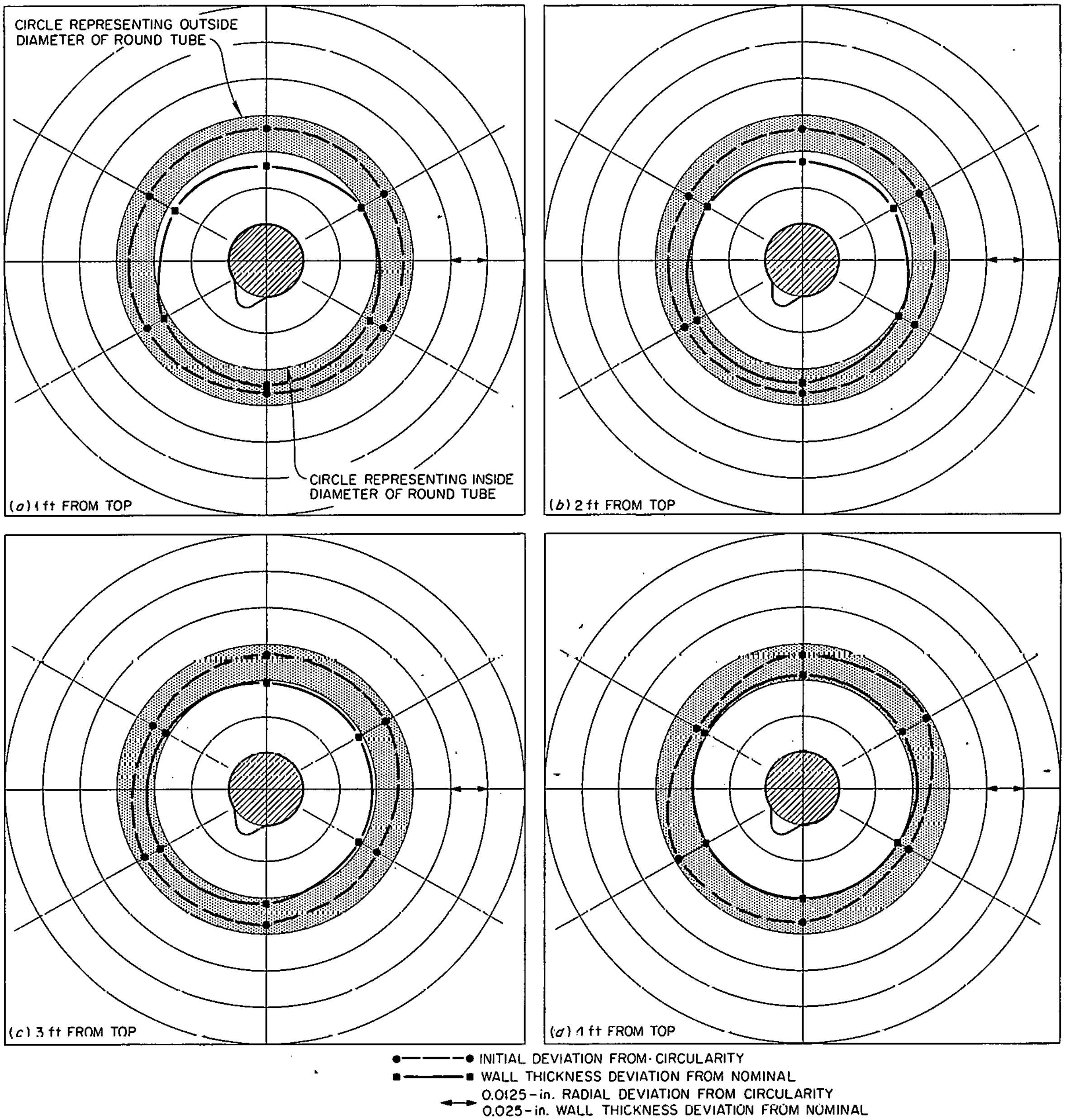

Fig. 13. Exaggerated Initial Dimensional Variations of Tube-Collapse Specimen UT-3.

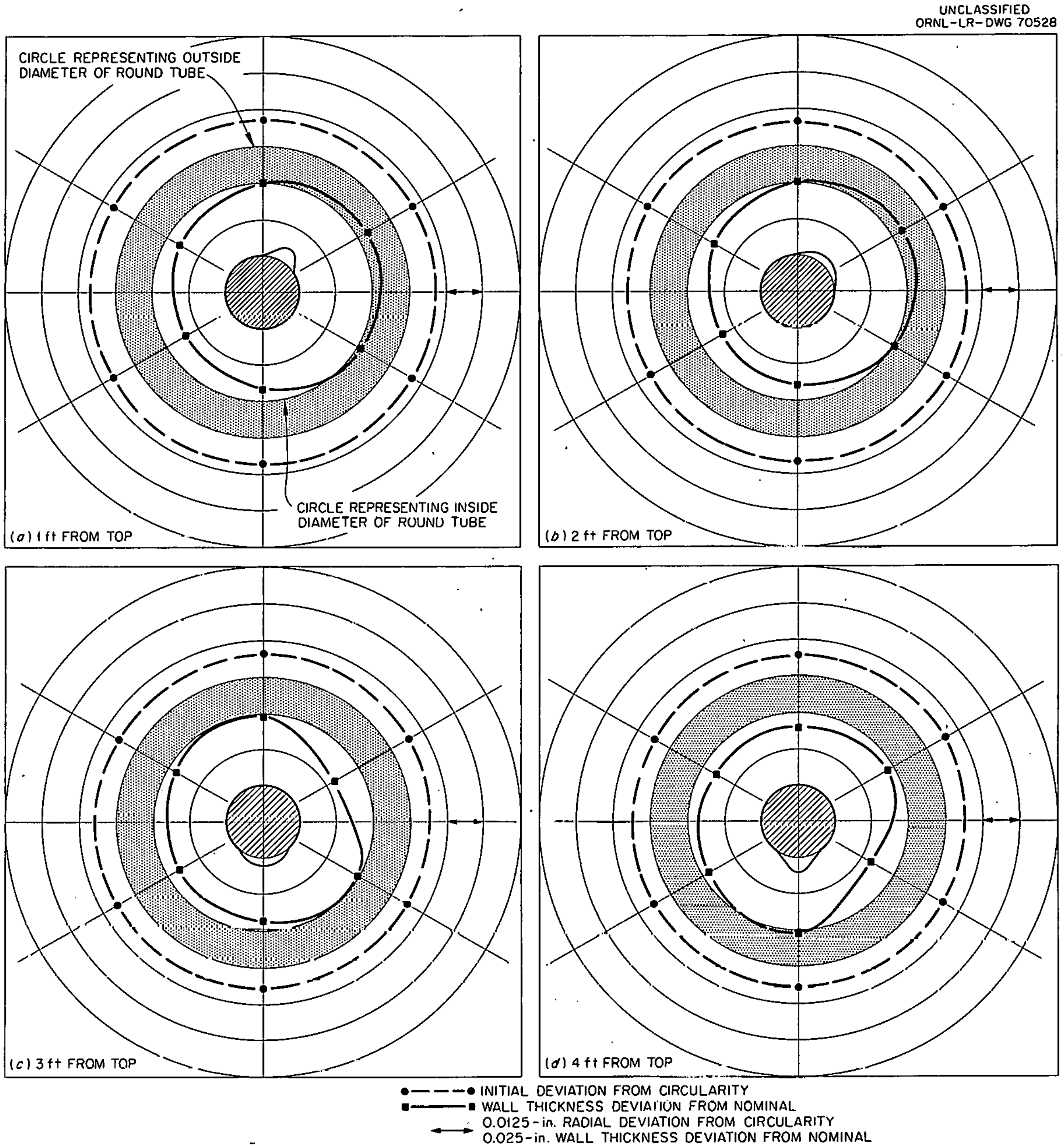

Fig. 14. Exaggerated Initial Dimensional Variations of Tube-Collapse Specimen UT-4.

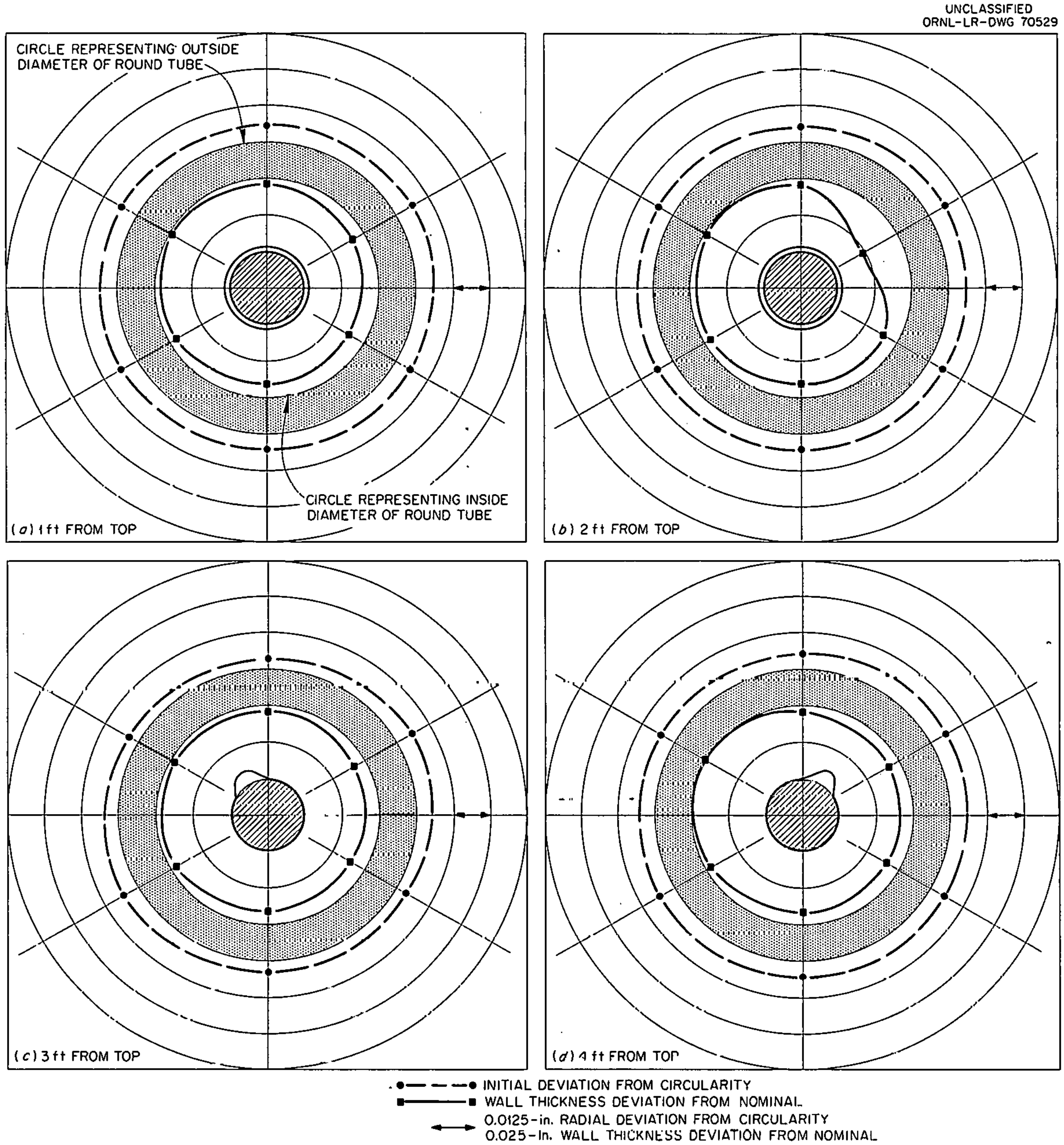

Fig. 15. Exaggerated Initial Dimensional Variations of Tube-Collapse Specimen UT-5.

UNCLASSIFIED
PHOTO 52812

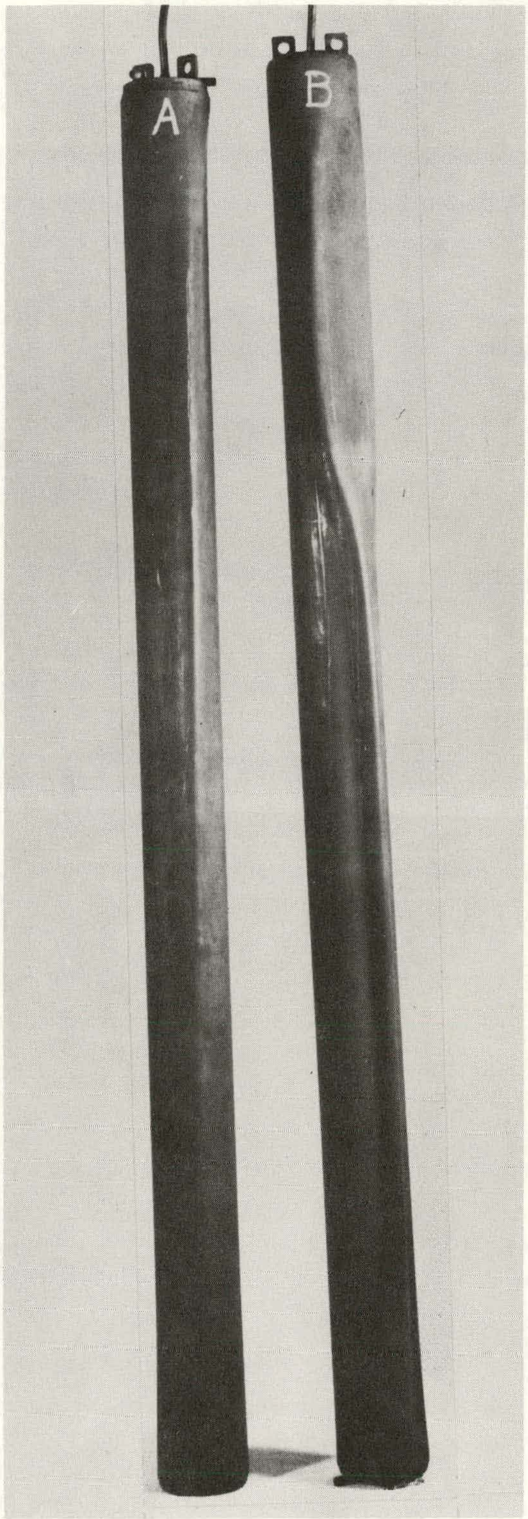

Fig. 16. Collapsed 4.0-in.-OD Specimens UT-1(B) and UT-2(A). Specimen A is a type 347 stainless steel tube and specimen B is a type 304 stainless steel tube.

continued to 680 hr, and, at the end of this time, the collapsed section extended axially along the specimen for a distance of approximately 1 ft.

The last tube in the series, UT-6 (see Table 3), was also subjected to an external pressure of 425 psi so that the test conditions duplicated those for UT-5. Several times during the test the specimen was removed from the vessel for a dimensional check, and the measurements were compared with those taken prior to testing. Although the ellipticity for this tube was much less apparent than for the other tubes, the same type of behavior was observed, with the initial ellipticity being magnified by creep of the material under an external pressure loading.

The initial variations in outside diameter and wall thickness, together with diameter variations measured at the end of 5710 hr, are shown in Fig. 17. The increase in ellipticity under test conditions may be clearly seen from this figure. During the test interruption at 5710 hr, a broken electrical lead for the failure-indicating system inside the tube was repaired. To make this repair, the lower end of the specimen was cut off and later rewelded. As a result, changes in the cross-sectional dimensions of the tube occurred, so measurements were again taken. The diameter variations obtained from the measurements taken before and after welding are plotted in Fig. 18, where it may be seen that only the lower cross section was significantly affected.

Figure 19 shows the variations in outside diameter and wall thickness obtained from measurements made after rewelding the tube at the end of 5710 hr, together with diameter variations after 11,310 hr. The plots in the figure again show that the deviation from circularity was increased during the time under load. The most pronounced change occurred at the lower cross section where the deviation from circularity after rewelding was decreased.

The change in the out-of-roundness factor was smaller during the first 5710 hr than during the next interval of 5600 hr between the test times of 5710 and 11,310 hr. This behavior differs from that observed for the 8.0-in.-OD specimen RD-4, described earlier, where the creep deformation was greater during the first 1056-hr time interval than the following interval of 1112 hr.

UNCLASSIFIED
ORNL-LR-DWG 70530

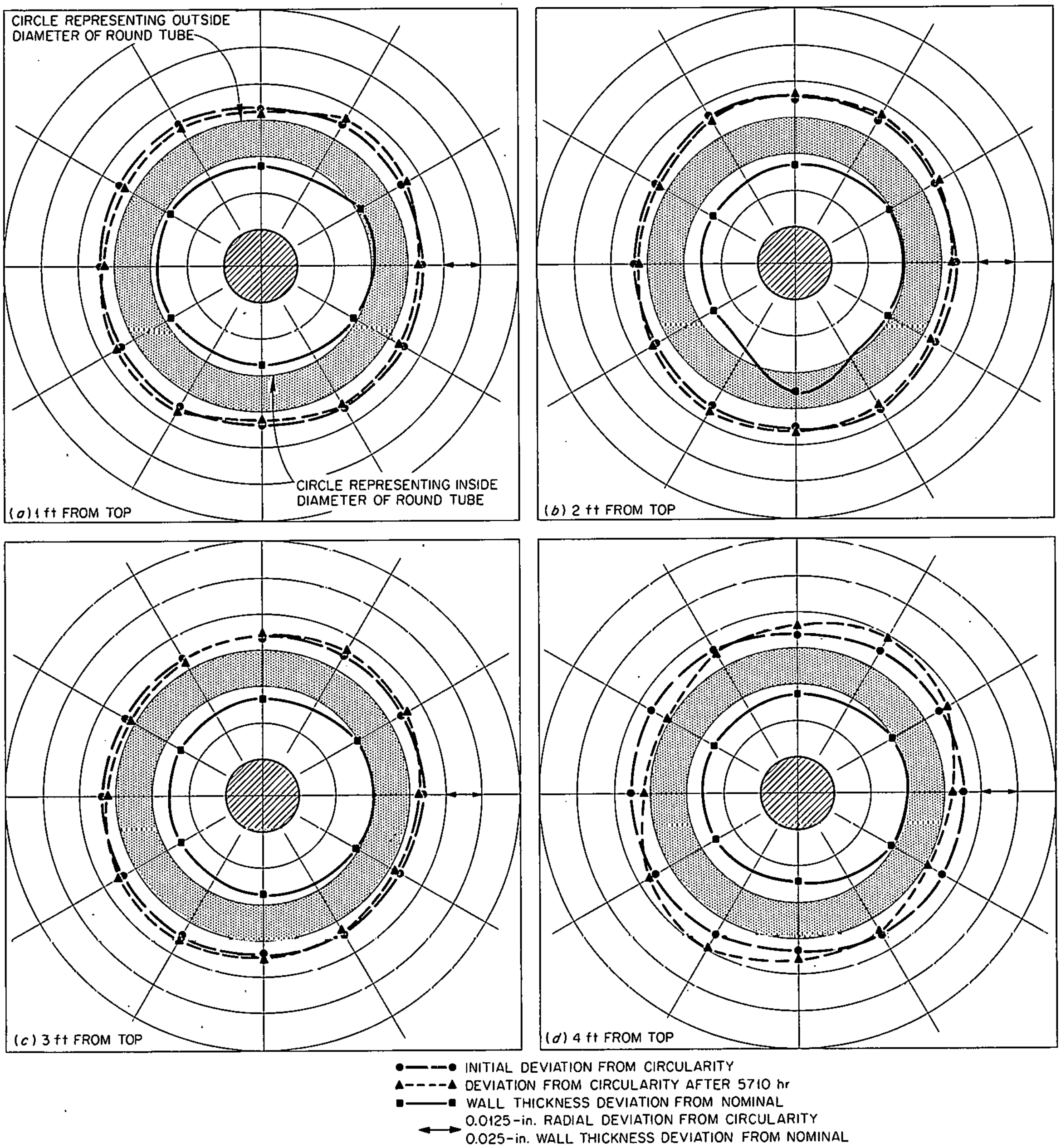

Fig. 17. Exaggerated Initial Dimensional Variations and Variations After 5110 hr for Tube-Collapse Specimen UT-6 Subjected to an External Pressure of 460 psi at 1200°F.

UNCLASSIFIED
ORNL-DWG 63-3831

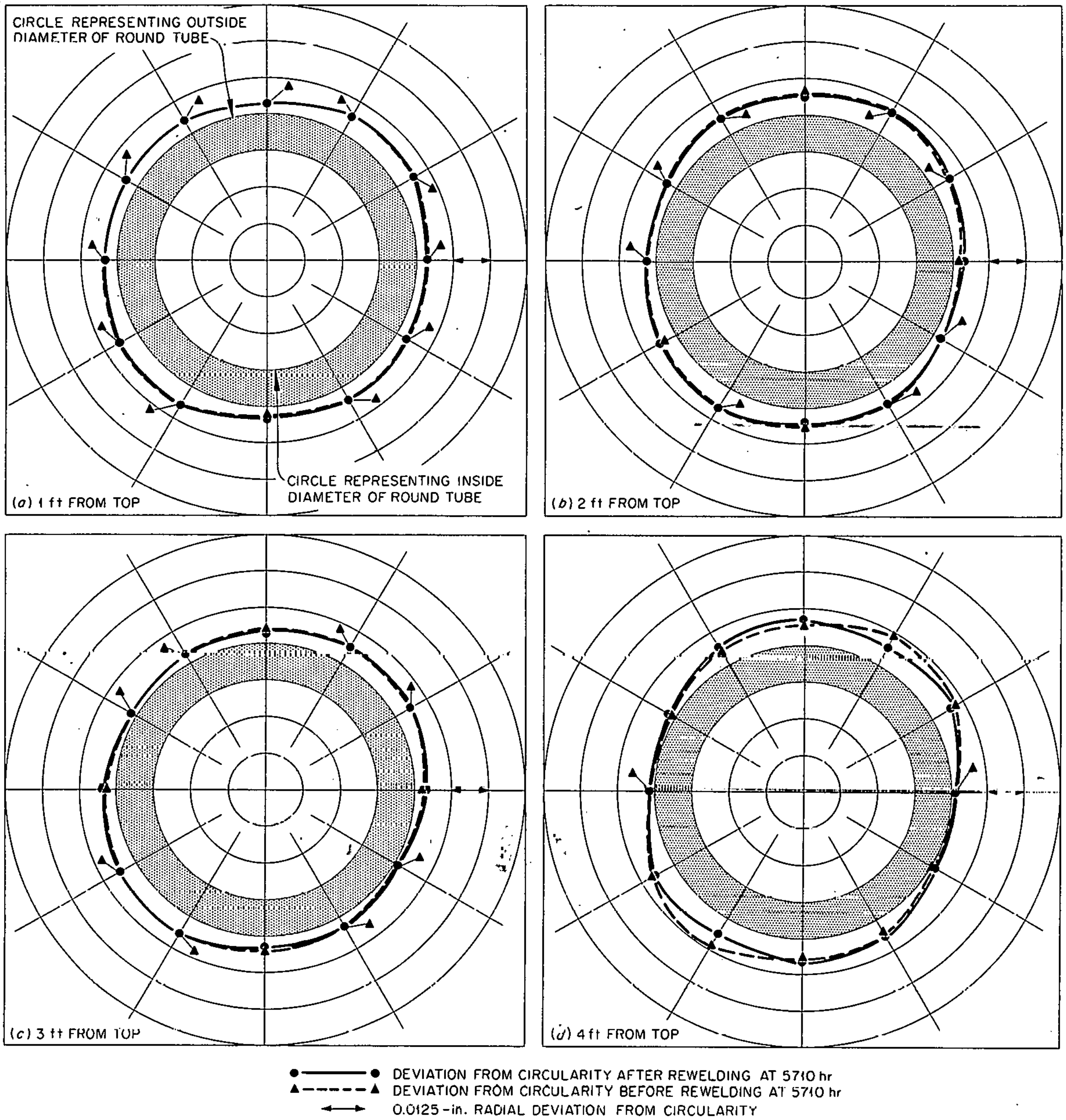

Fig. 18. Dimensional Variations of Specimen UT-6 Before Removing and After Rewelding End Cap at End of 5710 hr of Test.

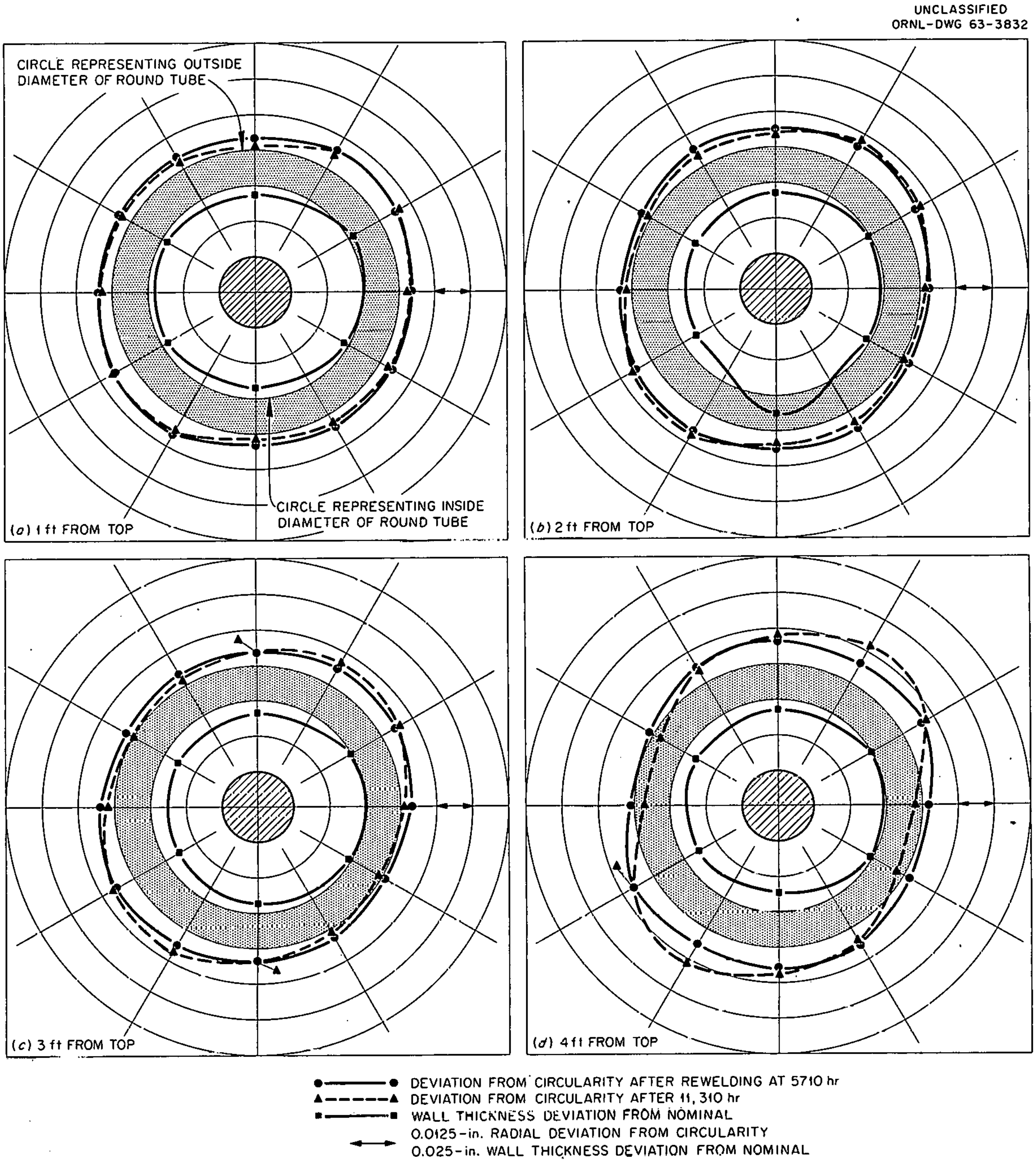

Fig. 19. Dimensional Variations of Specimen UT-6 After Rewelding at 5710 hr and Variations after 11,310 hr.

At the end of 14,160 hr, small increases in the out-of-roundness at each cross section were observed. The dimensional changes were small, but, at the orientations where the diameters were a maximum or minimum, the diameter changes appeared to be almost linear functions of time over the 5710- to 14,160-hr time interval. The variations in outside diameter at the end of 14,160 hr are not shown in this report, however, since there are only small differences between these variations and those at 11,310 hr.

Discussion of Results

The results from all the tests are shown in Fig. 20, which is a diagram of critical pressure versus time. Since this is a semilog plot the instantaneous-collapse data were placed at the 1-hr interval for convenience. Each point is labeled with the specimen number followed by the

UNCLASSIFIED
ORNL-DWG 64-1039

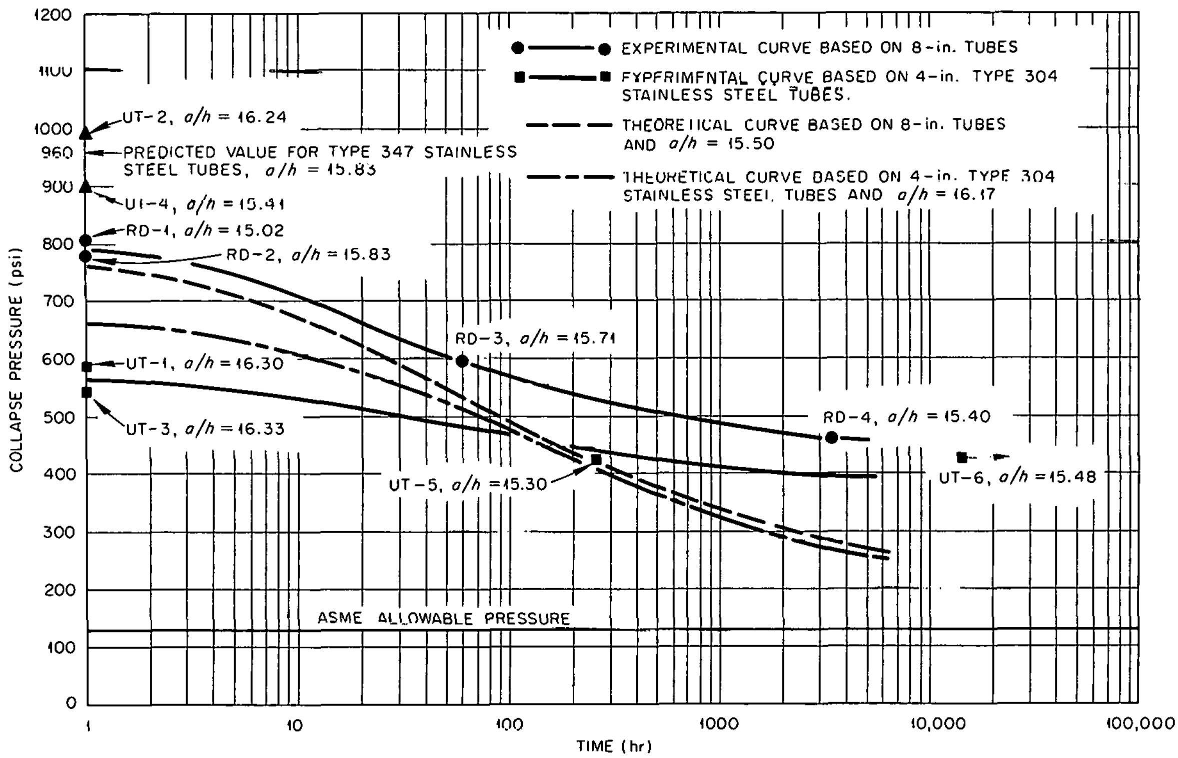

Fig. 20. Experimental Results and Comparisons with Theoretical Predictions and ASME Allowable Pressure.

mean radius-to-thickness ratio, a/h, for that particular tube. Although the four tubes in each case do not represent an adequate sample of time-dependent collapse behavior, smooth curves were drawn through the data for each size of type 304 stainless steel tube.

From these curves, the reductions in collapse pressure with time may be seen. The decrease in collapse pressure is fairly rapid at first, followed by an apparent leveling off. The data from the 4.0-in.-OD specimens indicate that very little decrease occurs with time after the first few hundred hours. Finally, the curve for the 8.0-in.-OD specimens approaches that for the 4.0-in.-OD ones for the maximum test times.

The collapse pressures for the type 347 stainless steel tubes were much higher than for the type 304 stainless steel units. The differences seen are due both to differences in material properties and lower test temperatures for the type 347 stainless steel specimens. However, because of the temperature variations along the length of the type 347 tubes, it is very difficult to estimate the effective temperatures at which they collapsed. Figure 20 also indicates that the 4.0-in.-OD type 304 stainless steel tubes collapsed at lower pressures than the 8.0-in.-OD tubes. This is due to the lower a/h ratio of the 4.0-in. tubes and to the differences in material properties between the two series.

Compressive stress-strain diagrams were obtained from sheet specimens that were cut from an undeformed portion of several tubes which were collapsed instantaneously. Three separate compressive stress-strain diagrams were obtained at a test temperature of 1200°F for each of the three series of tube specimens. A representative curve for each of the series is shown in Fig. 21. The figure shows that the material of the type 347 stainless steel tubes was considerably stronger than that of the type 304 stainless steel tubes. In addition, the material for the 8.0-in.-OD type 304 stainless steel tubes was slightly stronger than that of the 4.0-in.-OD type 304 stainless steel.

The curves in Fig. 21, together with isochronous creep curves for type 304 stainless steel, were used in connection with the tangent-modulus method to predict the instantaneous-collapse pressure for the type 347 stainless steel tubes and the instantaneous and time-dependent collapse behavior

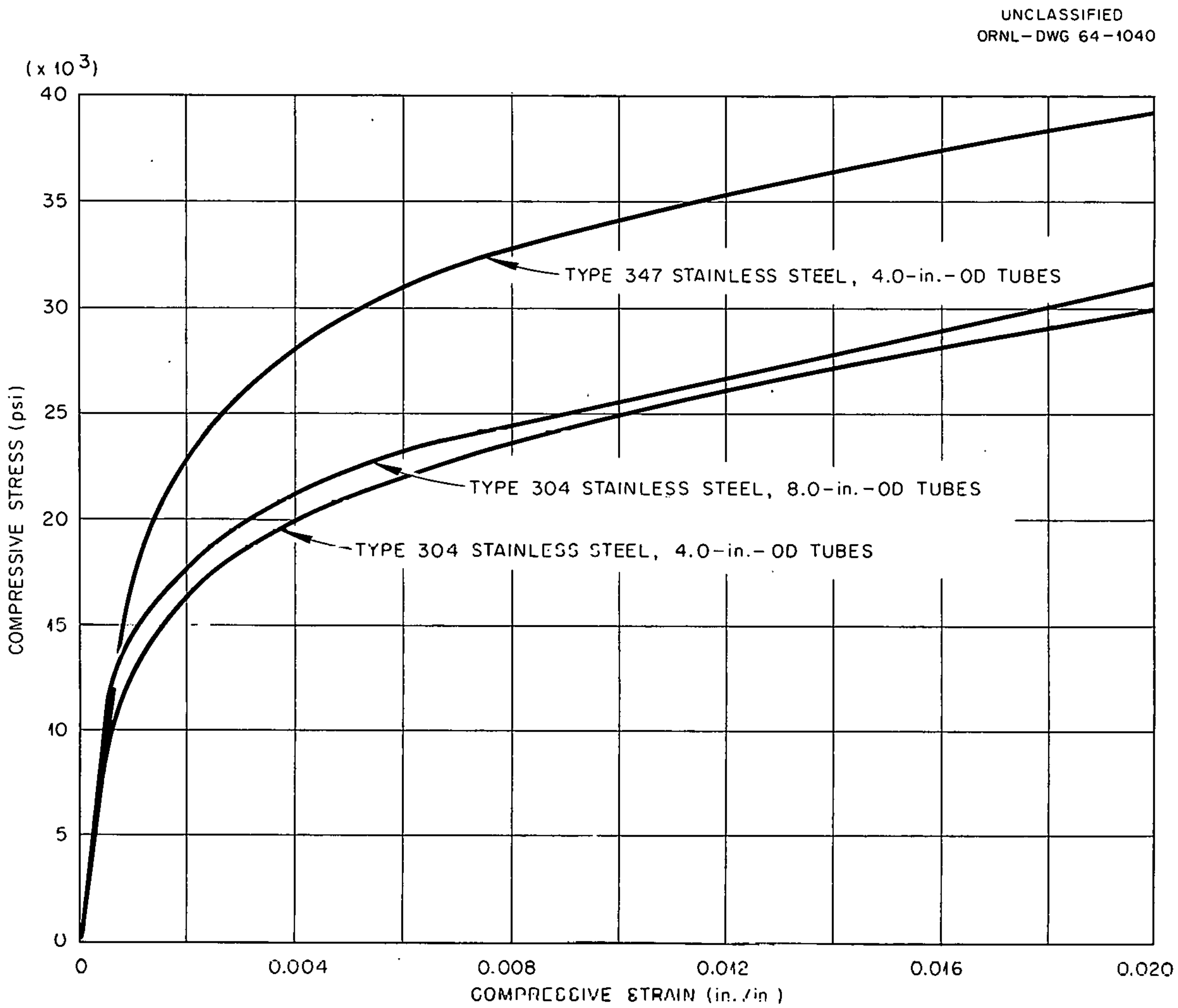

Fig. 21. Short-Time Compressive Stress-Strain Diagrams for Specimen Materials at 1200°F.

of the type 304 stainless steel tubes. The tangent-modulus method is discussed in ref. 1 and is illustrated in Figs. 16 and 17 of that report. The theoretical predictions for the type 304 stainless steel tubes are shown by the dashed curves in Fig. 20. The predicted collapse pressure for the type 347 stainless steel tube is also indicated. The two curves were calculated for the 8.0-in.-OD and 4.0-in.-OD tubes using mean radius-to-thickness ratios of 15.50 and 16.17, respectively. The tangent-modulus predictions are based on geometrically perfect tubes. Theoretical predictions, which take the initial out-of-roundness into consideration, are given for the 8.0-in.-OD tubes.[1] The predicted collapse pressure, 960 psi, for the type 347 stainless steel tubes agrees well with the two experimental points. The curve for the 8.0-in.-OD tubes falls below the experimental curve, and the differences between the two curves increase with time. In the case of 4.0-in.-OD tubes, the theoretical curve lies above the experimental one for relatively short times, but it falls below for times greater than a few hundred hours. The calculated curves tend to merge with time, and they display a fairly rapid decrease in pressure for short times, followed by a leveling off. All these general characteristics are similar to those ascribed to the experimental curves. One important feature of the calculated curves is the conservatism associated with them for relatively long time periods.

The straight line along the bottom of Fig. 20 corresponds to the allowable external pressure for tubes of both sizes according to ASME Boiler and Pressure Vessel Code Section VIII, Rules for Construction of Unfired Pressure Vessels. The ratio of experimental values to the Code value ranges from about 6.0 for instantaneous buckling to 58% of that factor (or ~3.4) at 3400 hr, in the case of the 8.0-in.-OD tubes. For the 4.0-in.-OD specimens the ratio of about 4.5 for instantaneous buckling is near the minimum to be expected from the use of the Code, but the decrease with time is less than in the case of the 8.0-in.-OD tube, with the ratio being 75% of the maximum value (~3.4), even after a few thousand hours.

It may be seen that the ASME Code gives conservative results for cases described in this report, even when time-dependent collapse may occur. When the amount of conservatism indicated cannot be tolerated, theoretical predictions may be used as a basis for design. For times of about 10,000 hr, the experimental curves yield a critical pressure ~1.7 times greater than the predicted value, instead of a factor of ~3.4, as in the case of the ASME Code allowable value. However, recourse to either model or prototype testing is necessary when optimization between wall thickness and external load-carrying abilities is required, such as in the case of nuclear reactors where poisoning effects or irradiation heating or both must be minimized.

The theoretical analyses[1] showed that out-of-roundness is a major factor in determining the collapse pressure, a fact borne out by the results of the experimental investigations using 8.0-in.-OD specimens. The calculated out-of-roundness factors for the larger tubes were greater than for the smaller ones, so the role of the out-of-roundness factor was more easily discernible in the first case. However, in the case of the 4.0-in. tubes the wall thickness variation was important, as evidenced by the tendency for the thinner section of the wall to move outward to form the lobe in each instance.

Maximum out-of-roundness factors and wall-thickness variations that could result from the dimensional tolerances allowed by the ASTM specifications pertaining to the stock for the specimens were calculated. These calculations were based upon the nominal tube dimensions, and the quantities are given in Table 5.

Table 5. Dimensional Variations Allowed by ASTM Specifications

	8-in.-OD Specimen	4-in.-OD Specimen
Material specification	ASTM-A213-58T	ASTM-A312-58T
Nominal wall thickness, in.	0.250	0.120
Maximum out-of-roundness factor	0.040	0.129
Positive wall-thickness variation, %	22	
Negative wall-thickness variation, %	0	12.5

A comparison of the data in this table with that given in Tables 1 through 4 shows that the maximum out-of-roundness factors for specimens RD-2 and RD-3 are greater than the values calculated from the specification, while those for the 4.0-in.-OD specimens (UT-1 through -6) are well within the calculated limit. In addition the minimum wall-thickness variations for the 8.0-in.-OD tubes are all less than the minimum values, as determined from the specifications. From these observations and the buckling characteristics of the tubes, the collapse pressures for the 8.0-in.-OD tubes tested are lower than those which would be expected from tubes of the same nominal dimensions where the stock meets ASTM-A213-58T specifications.

The reason for a longer life in the case of UT-6 compared with that for UT-5 is not understood. The dimensional data in Table 2 indicate that the reverse should be true. The locations of the maximum dimensional variations and the areas they cover may be just as important as the magnitudes. However, the tendency toward time independence of the collapse pressure, where very long times are involved, makes any interpretation difficult.

Appendix

Application to the EGCR Through-Tubes

The through-tubes for the experimental loops in the Experimental Gas-Cooled Reactor (EGCR)[2] pass through the reactor coolant outlet plenum and the core region. Thus they will be exposed to the highest temperature condition in the reactor. The operating conditions for the loops are such that two types of tube failure can occur; these are creep rupture from internal pressure and buckling from external pressure. The time to rupture may be predicted from tube-burst data. The instantaneous and creep-buckling characteristics are much more difficult to predict, however, and the experimental investigation described in this report was conducted to provide both instantaneous and time-dependent collapse data applicable to the experimental through-tubes.

In specifying the test program, a test temperature of 1200°F was selected, since the reactor is to have operating capability at this gas-outlet temperature. It was assumed that the useful life for a through-tube would be three years (26,280 hr) and that a tube would have to withstand an external pressure loading equal to the pressure in the primary coolant circuit of the reactor (~300 psi) for about 10% of the total lifetime (~2600 hr).

Although the four tubes tested in each set do not represent an adequate sample of time-dependent collapse behavior, significant conclusions may be drawn from the results. These results are again summarized in Fig. 22. An examination of the figure indicates that, for the particular 8.0-in.-OD tubes tested, an external pressure of 465 psi would produce collapse after the specified 2600 hr. This pressure is 155% of the actual 300-psi external pressure which will be imposed. The data for 4.0-in.-OD specimens yield similar results.

---

[2] "Final Hazards Summary Report," Vol. 1, Oak Ridge Operations Office, ORO-586, pp. 4–114, Oct. 10, 1962.

UNCLASSIFIED
ORNL-DWG 64-1041

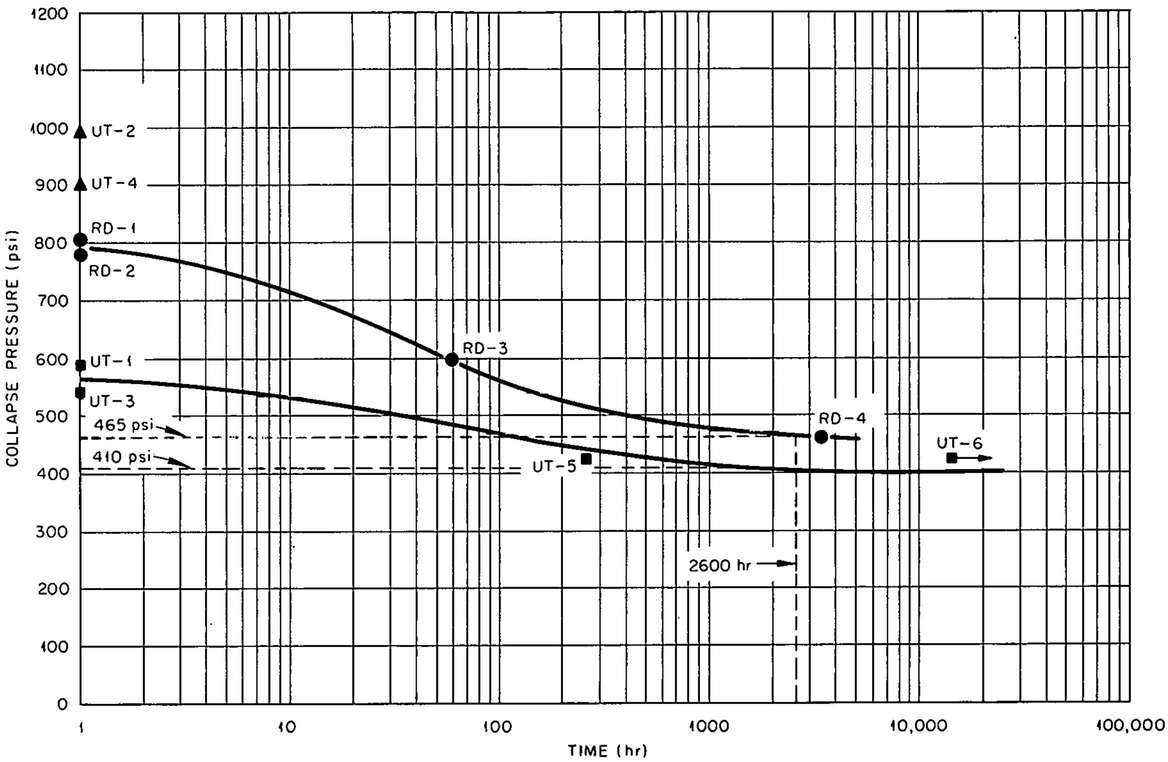

Fig. 22. Experimental Results from Buckling Program.

The through-tubes for the reactor are to be type 347 stainless steel rather than the type 304 stainless steel tested, and they were sized in accordance with the requirements of the ASME Code for vessels subjected to external pressure. The allowable pressures specified by the Code are less than 25% of the minimum observed instantaneous collapse pressures. Figure 20 indicates, however, that the pressure specified by the Code is about 30% of the external pressure that produces collapse after 2600 hr. Thus, assuming that type 347 stainless steel tubes behave similarly to type 304 stainless steel tubes, the Code-designed units will satisfactorily resist creep collapse during the specified time period.

Acknowledgements

The authors wish to acknowledge the participation and contributions of several individuals in the tube-collapse studies. The test facility for the 8.0-in.-OD tubes was developed with the assistance of J. C. Amos, who also tested the first specimen. J. E. Smith, with the aid of H. D. Curtis, was responsible for conducting the remaining tests on the 8.0-in.-OD specimens.

The 4.0-in.-OD tubes were tested at The University of Tennessee. Professors R. L. Maxwell and R. W. Holland of the Mechanical Engineering Department were responsible for designing and developing the furnace used and for conducting the experimental work. The experimental work at U. T. was done under Subcontract 875.

ORNL-3555

UC-80 – Reactor Technology
TID-4500 (26th ed.)

Internal Distribution

1. R. E. Adams
2. S. E. Beall
3. E. J. Breeding
4. C. A. Burchsted
5. C. J. Claffey
6. W. G. Cobb
7. C. W. Collins
8. J. M. Corum
9. D. A. Douglas
10. A. P. Fraas
11. W. R. Gall
12. A. Goldman
13–22. B. L. Greenstreet
23. N. Hilvety
24. F. T. Howard
25. H. G. MacPherson
26–46. W. D. Manly
47. W. R. Martin
48. H. A. McLain
49. S. E. Moore
50. S. A. Rabin
51. H. W. Savage
52. A. W. Savolainen
53. R. W. Schneider
54. M. J. Skinner
55. T. Sliski
56. D. B. Trauger
57. J. T. Vernard
58. J. R. Weir
59. J. H. Westsik
60. F. J. Witt
61. F. C. Zapp
62–64. Central Research Library
65–67. Y-12 Document Reference Section
68–91. Laboratory Records Department
92. Laboratory Records, RC

External Distribution

93. E. O. Bergman, National Engineering Science Co., Pasadena, California
94. A. I. Chalfant, Pratt & Whitney Aircraft
95. W. E. Crowe, Los Alamos Scientific Laboratory
96. R. M. Evan-Iwanowski, Syracuse University, Syracuse, N. Y.
97. R. W. Holland, University of Tennessee
98. B. F. Langer, Bettis Plant, Westinghouse, Pittsburgh, Penn.
99. Ralph Papirno, Aracon Laboratories, Concord, Mass.
100. W. A. Shaw, Auburn University, Auburn, Alabama
101. H. Lawrence Snider, Lockheed Aircraft Corporation, Marietta, Georgia
102. K. N. Tong, Syracuse University, Syracuse, N. Y.
103. J. N. Walker, DuPont Company, Aiken, South Carolina
104–106. P. D. Bush, Kaiser Engineers
107. R. A. Charpie, UCC Research Administration, New York, N. Y.
108. W. R. Cooper, Tennessee Valley Authority
109–110. D. F. Cope, Reactor Division, AEC, ORO
111–112. R. W. Coyle, Vallecitos Atomic Laboratory

113. E. Creutz, General Atomic
114-116. R. B. Duffield, General Atomic
117. H. L. Falkenberry, Tennessee Valley Authority
118. D. H. Fax, Westinghouse Atomic Power Division
119. M. Janes, National Carbon Research Laboratories, Cleveland, Ohio
120. T. Jarvis, Ford Instrument Company
121. James R. Johnson, Minnesota Mining and Manufacturing Company, Saint Paul, Minn.
122. Richard Kirkpatrick, AEC, Washington
123. C. W. Kuhlman, United Nuclear Corp.
124-125. H. Lichtenburger, General Nuclear Engineering Corp.
126-128. S. Matovich, Allis-Chalmers Mfg. Co.
129. J. P. McGee, Bureau of Mines, Appalachian Experiment Station
130. R. W. McNamee, UCC Research Administration, New York, N. Y.
131. R. E. Pahler, Reactor Division, AEC, Washington
132. H. B. Rahner, Savannah River Operations Office
133. Corwin Rickard, General Atomic
134. M. T. Simnad, General Atomic
135. Nathanial Stetson, Savannah River Operations Office
136. Donald Stewart, AEC, Washington
137. S. A. Szawlewiez, AEC, Research and Development Branch, Division of Reactor Development
138. Philip L. Walker, Pennsylvania State University
139. R. E. Watt, Los Alamos Scientific Laboratory
140-141. W. L. Webb, East Central Nuclear Group, Inc.
142. C. E. Winters, UCC, Cleveland, Ohio
143. Lloyd R. Zumwalt, General Atomic
144. Division of Research and Development, AEC, ORO
145-756. Given distribution as shown in TID-4500 (26th ed.) under Reactor Technology category (75 copies - OTS)